Development of an Orally Available and Central Nervous System (CNS)-Penetrant *Toxoplasma gondii* calcium-dependent protein kinase 1 (*Tg*CDPK1) Inhibitor with Minimal Human Ether-à-go-go-Related Gene (hERG) Activity for the Treatment of *Toxoplasmosis*

Rama Subba Rao Vidadala[§], **Kasey L. Rivas**[‡], **Kayode K. Ojo**[‡], **Matthew A. Hulverson**[‡], **Jennifer A. Zambriski**[€], **Igor Bruzual**[¶], **Tracey L. Schultz**[&], **Wenlin Huang**[†], **Zhongsheng Zhang**[†], **Suzanne Scheele**[#], **Amy E. DeRocher**[#], **Ryan Choi**[‡], **Lynn K. Barrett**[‡], **Latha Kallur Siddaramaiah**[†], **Wim G. J. Hol**[†], **Erkang Fan**[†], **Ethan A. Merritt**[†], **Marilyn Parsons**[#,^], **Gail Freiberg**[λ], **Kennan Marsh**[λ], **Dale Kempf**[λ], **Vern B. Carruthers**[&], **Nina Isoherranen**[‖], **J. Stone Doggett**[¶], **Wesley C. Van Voorhis**[‡,^,*], and **Dustin J. Maly**[§,†,*]

[†]Department of Biochemistry, University of Washington, Seattle, WA 98195, United States

[‡]Department of Medicine, Division of Allergy and Infectious Diseases, and the Center for Emerging and Re-emerging Infectious Diseases (CERID), University of Washington, Seattle, WA 98109, United States

[§]Department of Chemistry, University of Washington, Seattle, WA 98195, United States

[#]Center for Infectious Disease Research (formerly Seattle Biomedical Research Institute), Seattle, WA 98109, United States

[^]Department of Global Health, University of Washington, Seattle, WA 98195 United States

[¶]Portland VA Medical Center, Portland, OR 97239, United States

[€]Paul G. Allen School for Global Animal Health, College of Veterinary Medicine, Washington State University, Pullman, WA 99164, United States

[&]Department of Microbiology and Immunology, University of Michigan Medical School, Ann Arbor, MI 48109 United States

[‖]Department of Pharmaceutics, University of Washington, Seattle, WA 98195, United States

λAbbVie, N. Chicago, Illinois 60064, United States

Abstract

New therapies are needed for the treatment of toxoplasmosis, which is a disease caused by the protozoan parasite *Toxoplasma gondii*. To this end, we previously developed a potent and selective inhibitor (compound **1**) of *Toxoplasma gondii* calcium-dependent protein kinase 1 (*Tg*CDPK1) that possesses anti-toxoplasmosis activity *in vitro* and *in vivo*. Unfortunately, **1** has potent human Ether-à-go-go-Related Gene (hERG) inhibitory activity, associated with long Q-T syndrome, and, consequently, presents a cardiotoxicity risk. Here, we describe the identification of an optimized *Tg*CDPK1 inhibitor **32**, which does not have a hERG liability and possesses a favorable pharmacokinetic profile in small and large animals. **32** is CNS-penetrant and highly effective in acute and latent mouse models of *T. gondii* infection, significantly reducing the amount of parasite in the brain, spleen, and peritoneal fluid and reducing brain cysts by >85%. These properties make **32** a promising lead for the development of a new anti-toxoplasmosis therapy.

Graphical abstract

1
T. gondii EC$_{50}$: 140 nM
AUC: 430 μM.min
hERG: 0.40 μM

32
T. gondii EC$_{50}$: 60 nM
AUC: 13,700 μM.min
hERG: >10 μM
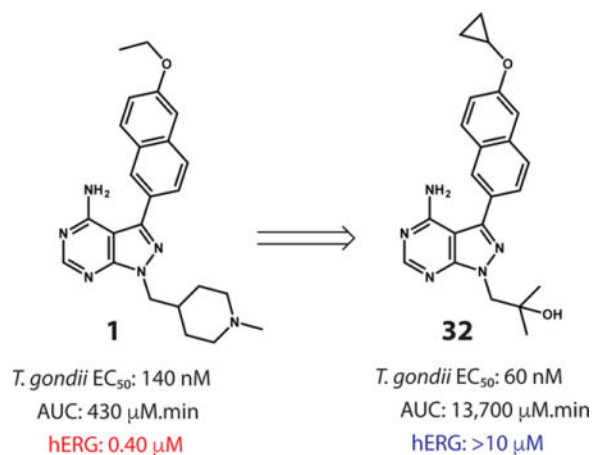
Introduction

Toxoplasmosis is an infectious disease that results from the infection of the protozoan parasite *Toxoplasma gondii*.[1] While cats are the definitive host of *T. gondii*, this zoonotic parasite is estimated to be one of the most prevalent in humans, with approximately 30–50% of the world's population being seropositive.[2] *T. gondii* infections of humans can be caused by the consumption of undercooked meat containing tissue cysts or by the accidental ingestion or inhalation of oocysts from cat feces.[1,3] *T. gondii* parasites rapidly proliferate during acute infection before being controlled by the immune system in immunocompetent individuals.[4] However, despite this robust immune response, the *T. gondii* parasite is not eliminated. Instead, the parasite transforms into a slowly dividing cellular stage called the bradyzoite, which cluster into tissue cysts mainly located in the brain, eyes, and striated muscle.[5] Tissue cysts can persist for the lifetime of the host; periodically rupturing and releasing tachyzoites that can again rapidly replicate and reform cysts. While in immunocompetent individuals toxoplasmosis is usually asymptomatic and recovery occurs

in the absence of antibiotic treatment, *T. gondii* infection can sometimes trigger severe retinal diseases, which has been recently recognized to be particularly prevalent in regions of South America.[6,7] When *T. gondii* infection occurs during pregnancy, vertical transmission can ensue, resulting in birth defects or miscarriage.[8] For individuals with compromised immune systems, active *T. gondii* infection primarily leads to encephalitis or chorioretinitis, but may cause disease in other organs as well.[9]

Current first-line therapy for toxoplasmosis involves treatment with a combination of pyramethamine and sulfadiazine, which inhibit the folate pathway in *T. gondii*.[10] However, this therapeutic regimen requires long dosing periods and can be limited by rash, leukopenia, nephrotoxicity, teratogenicity, and kernicterus in newborns.[11] There is a longstanding need for better toxoplasmosis drugs, especially therapeutic agents that are non-toxic, nonteratogenic, and with simple dosing profiles.

In order to develop new therapies for the treatment of toxoplasmosis, we and others have explored strategies that involve inhibiting enzymatic components of calcium-dependent cellular processes in the parasite, which are necessary for invasion into and egress from host cells. *T. gondii* calcium-dependent protein kinase 1 (*Tg*CDPK1) is a particularly promising target due to its role in gliding and motility.[12] Gliding and motility are necessary for *T. gondii* invasion and egress, and as *T. gondii* is an obligate intracellular parasite that requires these processes to proliferate, inhibition of *Tg*CDPK1 represents a promising new anti-parasitic strategy. Indeed, genetic or pharmacological disruption of *Tg*CDPK1 function blocks parasite growth *in vitro* and is able to prevent and treat established *T. gondii* infections in mice.[13–20]

We previously developed a number of highly promising pyrazolopyrimidine (PP)-based ATP-competitive inhibitors that are able to potently block the enzymatic activity of *Tg*CDPK1. These selective *Tg*CDPK1 inhibitors are able to block the invasion of *T. gondii* into host cells, preventing proliferation of the parasite.[15,19,20] Recently, we have demonstrated that the *Tg*CDPK1 inhibitor **1** (1294) is an orally available inhibitor that possesses anti-toxoplasmosis activity *in vitro* and *in vivo*, with no apparent signs of toxicity.[15] Furthermore, **1** was able to block vertical transmission of *Neospora caninum* in a pregnant mouse model, and since *N. caninum* is closely related to *T. gondii*, it speaks to a potential therapeutic application for toxoplasmosis in pregnancy.[21,22] Unfortunately, we have found that **1** has potent human Ether-à-go-go-Related Gene (hERG) inhibitory activity[23]–associated with long Q-T syndrome–and, thus, presents a significant cardiotoxicity risk in humans.[24] Here, we describe the identification of optimized PP-based *Tg*CDPK1 inhibitor **32**, which does not have an hERG liability but possesses the favorable anti-parasitic activity of lead compound **1**.

Results and Discussion

Molecular Design and Synthesis

*Tg*CDPK1 contains a *C*-terminal calcium-binding domain of 4 EF-hands (CDPK activation domain) linked to an *N*-terminal kinase domain. The ATP-binding cleft of *Tg*CDPK1, which is the site of interaction with PP-based inhibitors, is similar in structure to mammalian

protein kinases with the exception that it contains a rare glycine residue at the gatekeeper position. The starting point for this study was compound **1**, which is based on a PP scaffold that forms two hydrogen-bonding interactions with the hinge region of TgCDPK1 (Figure 1). The C-3 (R_1) position of **1** is derivatized with a bulky 6-ethoxy-2-naphthyl group that occupies a hydrophobic pocket adjacent to TgCDPK1's glycine gatekeeper residue. As glycine is a very uncommon gatekeeper residue, the space occupied by the 6-ethoxy-2-naphthyl group provides a means to obtain high selectivity over mammalian kinases, which often have larger gatekeepers that constrain access to the hydrophobic back pocket. The 6-alkoxy-2-naphthyl substitution pattern appears to be optimal for complementing the hydrophobic gatekeeper pocket of TgCDPK1 and enhancing overall inhibitor selectivity. At the N-1 position, **1** contains an N-methyl-4-piperidinemethylene group, directed toward the sugar pocket. This basic group increases potency for TgCDPK1 and, in combination with 6-alkoxy-2-naphthyl substituents at the C-3(R_1) position, the 4-piperidinemethyl group greatly enhances kinase selectivity.[25]

Several synthetic strategies were used to generate derivatives of **1**. The synthetic route shown in Scheme 1 was used to generate inhibitors that contain a 6-ethoxy-2-naphthyl group at the R_1 position and various 4-piperidinemethylene or 3-azetidinemethylene derivatives at the R_2 position (Table 1). Inhibitors that contain an N-methyl-4-piperidinemethylene R_2 group and various 6-alkoxy-2-naphthyl or 6-alkoxy-2-quinolinyl groups at the R_1 position were generated by either alkylation of t-butyl-4-((4-amino-3-(6-hydroxynaphthalen-2-yl)-1H-pyrazolo[3,4-d]pyrimidin-1-yl)methyl)piperidine-1-carboxylate, followed by Boc deprotection and reductive alkylation, or by palladium-catalyzed Suzuki-Miyaura couplings between appropriate aryl boronic acids and boronate esters and t-butyl-4-((4-amino-3-iodo-1H-pyrazolo[3,4-d]pyrimidin-1-yl)methyl)piperidine-1-carboxylate, followed by Boc deprotection and reductive alkylation (Scheme 2). Boronic esters and boronic acids that are not commercially available were prepared from aryl bromides using standard methods.[26] Compounds containing variable groups at the R_2 position were generated by alkylating 3-iodo-1H-pyrazolo[3,4-d]pyrimidin-4-amine with alkyl halides, alkyl mesylates, or expoxides followed by Suzuki-Miyaura coupling to R_1-boronic acids or boronate pinacol esters (Scheme 3).

Inhibitor Testing Cascade

A multi-assay testing cascade was used to determine if newly generated analogs demonstrated superior anti-parasitic properties compared to compound **1**. Compounds were first tested for the ability to block the activity of recombinant TgCDPK1 using a luminescence-based assay that measures the consumption of ATP in the presence of the peptide substrate Syntide 2.[19] All assays were performed in the presence of 2 mM $CaCl_2$ and at an ATP concentration–10 μM–equal to TgCDPK1's Michaelis constant (K_m). Compounds of sufficient *in vitro* enzyme inhibitory activity were then tested for their ability to block the invasion and growth of parasites into human foreskin fibroblast cells using a previously described *T. gondii* cellular assay.[19] Inhibitors with comparable *in vitro* enzymatic and cellular potencies as **1**, were next screened for selectivity in two assays. To determine selectivity for TgCDPK1 over mammalian kinases, compounds were tested against the tyrosine kinase Src, which is representative of the most likely off targets of

pyrazolopyrimidine-based inhibitors that contain a large aryl group at the C-3 (R_1) position due to its small threonine gatekeeper residue.[27] General off target toxicity was determined by testing for growth inhibition (GI_{50}) of two mammalian cell lines, HepG2 (liver) and CRL-8155 (lymphoblast). As elimination of hERG activity was a major goal of this study, all compounds with favorable profiles were tested for hERG activity using a previously described assay.[23,28,29]

In generating analogs of **1**, we felt that it would be important to retain a 6-alkoxynaphthalen-2-yl group at the C-3 (R_1) position. In addition, due to the unexpected contribution of the 4-piperidinemethyl group to inhibitor potency and selectivity,[25] compounds that contain a similar substituent at the R_2 position were focused on first. Results for compounds containing a fixed 6-ethoxynaphthyl at the R_1 position and various 4-piperidinemethyl or 3-azetidinemethyl groups at the R_2 position are shown in Table 1. Increasing the size of the *N*-alkyl group on the 4-piperidinemethyl moiety (**7**) resulted in slightly reduced target potency and did not diminish hERG inhibition. Replacing the 1-methylpiperidin-4-ylmethyl group of **1** with either a 3-azetidinemethyl (**5**) or a 1-methyl-3-azetidinemethyl (**6**) group resulted in potent inhibition of *Tg*CDPK1, albeit with attenuated activity against parasite proliferation, but only a slight decrease in hERG inhibition. However, an analog containing an acetylated 4-piperidinemethyl group (inhibitor **8**) displayed acceptable levels of inhibition of the *Tg*CDPK1 enzyme and parasite proliferation with no hERG activity. Inhibitor **9**, which contains a 1-acetyl-3-azetidinemethylene group instead of a 1-acetyl-4-piperidinemethyl moiety, also lacks hERG activity but possesses unacceptably low activity in the *T. gondii* cellular assay. These results are consistent with the observed correlation between inhibitor basicity and hERG inhibition.[30–32]

We next explored whether hERG inhibition could be reduced in analogs of **1** that maintain the 1-methyl-4-piperidinemethyl group by modifying the *N*-1 position (R_2) of the pyrazolopyrimidine scaffold (Table 2). For the 6-alkoxynaphthalen-2-yl series, inhibitors containing cycloalkyloxy groups larger than ethyl (**10–12**) were potent *Tg*CDPK1 inhibitors and were of reasonable potency in the *T. gondii* cellular assay. However, the hERG activity of these compounds was comparable to **1**. Unfortunately, introduction of more polar groups at the 6 position of the naphthyl ring (**13–16**), which reduces overall inhibitor lipophilicity and would be expected to diminish hERG activity, led to less potent inhibition of *Tg*CDPK1 and subsequent reduced potency in the *T. gondii* cellular assay. A more favorable inhibitor profile was obtained by replacing the 6-ethoxy-2-naphthyl group of **1** with a 2-ethoxyquinolin-6-yl moiety (**17**). Inhibitor **17** showed comparable levels of *Tg*CDPK1 enzyme inhibition and efficacy in the invasion assay as **1**, with no detectable Src inhibition or mammalian cell toxicity. Compound **17** also possesses 25-fold lower activity against hERG than **1**. However, replacing the ethyl group of **17** with more hydrophobic substituents, like trifluoroethyl (**18**) or cyclopropyl (**19**), led to unacceptable levels of hERG inhibition (Table 2).

Finally, we investigated whether the cyclic amine substituent at the R_2 position of **1** can be replaced with another group that confers similar potency, selectivity, and solubility. We have previously shown that inhibitors possessing R_2 groups that are connected to the *N*-1 position of the PP scaffold through a methylene linkage demonstrate the highest degree of selectivity

for TgCDPK1 over mammalian kinases with small gatekeepers, like the tyrosine kinases Src and Abl.[25] Therefore, a panel of analogs with variable R_2 groups, which extend into the ribose-binding pocket of the ATP-binding site was generated (Table 3). In general, inhibitors of this class are potent inhibitors of the TgCDPK1 enzyme and efficacious in the $T.$ $gondii$ cellular assay. Furthermore, all of the inhibitors in Table 3 are highly selective (>150-fold) for TgCDPK1 over Src. Consistent with basicity at the R_2 position playing a major role in hERG inhibition, inhibitor **20**, which contains a dimethylamino group at the R_2 position, has a similar level of hERG activity as **1**. Compounds **21**–**23**, which all contain an isobutyl group at the R_2 position, are potent inhibitors of the TgCDPK1 enzyme and are at least as effective as **1** against the parasite. Importantly, these compounds are >3500-fold selective for TgCDPK1 over Src, demonstrate no detectable growth inhibition of HepG2 and CRL-8155 cells, and lack hERG activity. Compounds **24**–**29**, which all contain a cycloalkyl ether group linked to the N-1 (R_2) position through a methylene, are also effective inhibitors of TgCDPK1 and parasite proliferation. All of these compounds, except **28**, have an IC_{50} >10 μM for Src activity and do not inhibit the growth of mammalian cells. Furthermore, all of the inhibitors in this series, except **24** (IC_{50} = 1.9 μM), have an IC_{50} of greater than 10 μM for hERG activity. Inhibitors **30**–**36**, which either contain a 2-methylpropan-2-ol or a 2,2-dimethylpropan-1-ol group at the R_2 position also possess desirable profiles: potent TgCDPK1 enzyme inhibition, effective inhibition of parasite proliferation, and no detectable off-target inhibition or toxicity.

Pharmacokinetic Profiling of Potent and Selective TgCDPK1 Inhibitors

Based on the abilities of a number of inhibitors to potently block $T.$ $gondii$ proliferation in mammalian cells, while demonstrating little or no off-target toxicity or hERG inhibition, we next prioritized compounds based on their solubility in water and pharmacokinetic (PK) properties (Table 4). The aqueous solubility of inhibitors **8**, **17**, **29**, **31**–**34**, and **35** was determined at pH = 6.5. The initial PK profiles of these inhibitors were determined after a single 10 mg/kg oral dose in three Balb/c mice, with sampling conducted at the time points indicated in the Experimental Section. As a reference, after a 10 mg/kg *per os* (PO) dose, lead inhibitor **1** demonstrated a maximum concentration (C_{max}) of 0.75 ±0.15 μM and total exposure (area under the plasma concentrations versus time curve, AUC) of 430 ±84 μM·min. Inhibitors **29**, **34**, and **35** were poorly soluble (<20 μM) relative to **1** (solubility = 82 μM) and all three compounds had lower exposures and higher clearances than **1**. Inhibitors **8** and **17** demonstrated better solubility but also had a lower exposure and higher clearance than **1**, which is likely due to the more efficient metabolism of these compounds. In contrast, inhibitors **31**–**33**, which all contain a 2-methylpropan-2-ol at the R2 position, were highly soluble and **32** and **33** reached maximum serum concentrations (C_{max}) >10-fold higher and total exposure >30-fold higher than **1** (Table 4 and Figure 2). Compound **31** was absorbed rapidly with a T_{max} of 50 min and a C_{max} nearly 10-fold higher than **1**. Yet, the overall exposure of **31** was only twice as high as **1** and much lower than **32** and **33**. Based on this mouse pharmacokinetic data, compounds **32** and **33** were selected for further pharmacokinetic and tolerability studies.

Dose Finding and Tolerability of 32 and 33

Based on the PK parameters of **32** and **33** following single dose administration to mice, these compounds were evaluated for tolerability following escalated dosing. Both compounds were initially dosed at 10 mg/kg on day one. As no observable adverse effects were detected in mice dosed with either **32** or **33**, the next dose was increased to 50 mg/kg on day 4, followed by a final dose of 100 mg/kg on day 8. Mice showed no overt signs of toxicity or weight loss over the 10-day observation period. Next, the plasma protein binding of both compounds was evaluated. Both compounds were highly protein bound in mouse plasma with plasma protein binding of 96% for **32** and 88% for **33**. Based on the protein binding values the plasma concentrations required to maintain unbound plasma exposure above the TgCDPK1 EC_{50} are 1.33 μM for **33** and 1.5 μM for **32**. Using these target concentrations and the single dose PK data, a multiple dosing regimen with a loading dose of 20 mg/kg of **32** and **33** followed by a 5 mg/kg daily dose for five days was evaluated. Blood was collected at multiple time points to determine plasma concentrations over the course of treatment (Figure 3). Both compounds demonstrated excellent exposure through the 24-hour dosing interval with the trough concentrations remaining >1.5 μM throughout the study. The measured concentrations following multiple dosing were similar to those predicted from the single dose PK studies in mice (Figure 3). Neither compound showed any evident signs of toxicity compared to mice dosed with vehicle only. Cardiac puncture blood collection was performed at the end of the study for complete blood count and serum biochemical profiles. All results were reported by Phoenix Central Laboratory to be within a normal range for species and age.

In a second multiple dose study compound **32** was administered at 50 mg/kg PO every other day for 5 doses and compound **33** was administered with a 20 mg/kg loading dose followed by a 10 mg/kg maintenance dose every other day for 5 doses. The exposure to **33** with this dosing regimen was similar to the one observed with daily dosing of the lower dose and the plasma concentration at various time points were well predicted based on the single dose PK results. With compound **32** plasma concentrations remained >10 μM for the entire duration of the study (Figure 3) with maximum concentrations reaching 43 μM. The exposure to compound **32** following the last 50 mg/kg dose was higher than predicted from single dose studies with longer half-life suggesting possible saturation of metabolism at this dose.

Based on the favorable single and multiple dose PK and the lack of observable toxicity, compounds **32** and **33** were evaluated for tolerability and PK characteristics in rats following intravenous (IV) and PO dosing. Following IV administration to rats both **32** and **33** displayed biphasic kinetics with compound **33** reaching distribution equilibrium more rapidly than **32** (Figure 4). Compound **32** distributed approximately to total body water with a volume of distribution at steady state (V_{ss}) of 0.9 L/kg. The distribution of **33** was more extensive with a V_{ss} of 5.8 L/kg. Both compounds had very low systemic clearances in rats but, in contrast to mice, the clearance of **33** was 4-fold higher than that of **32**. The elimination half-lives of both compounds were acceptable for multiple dosing regimens, 9.6 and 13 hours for **32** and **33**, respectively (Figure 4).

Following oral administration to rats both compounds showed slow absorption with absorption phase continuing for 12 hours after oral dosing. The plasma concentrations over the 24-hour period after PO dosing exceeded those observed after IV dosing (Figure 4) suggesting that both **32** and **33** had essentially complete bioavailability in rats. The apparent bioavailability of these compounds was greatly improved compared to that of compound **1** (46%).

Because it is important that anti-toxoplasmosis therapies are able to prevent reactivation of parasites within tissue cysts, which largely reside in the central nervous system (CNS), the distribution of compounds **32** and **33** to the brain was next determined. To do this, the distribution of **32** and **33** into mouse brain (n=3) at one hour after intraperitoneal dosing of 5 mg/kg was measured. The mean concentration of compound **32** at one hour in brain was 1.2 ±0.5 μM, a concentration well above the TgCDPK1 EC_{50}. The corresponding plasma concentration of **32** was 4.1 ±1.1 μM resulting in a brain to plasma concentration ratio of **32** of 0.33 ±0.22. This brain penetration was comparable to **1** (0.31). In accordance with the larger distribution volume of compound **33**, it demonstrated a greater brain to plasma concentration ratio (1.65 ±0.84). Both the brain and plasma concentration of **33**, 1.90 ±0.24 μM and 1.23 ±0.76 μM, respectively, were above the TgCDPK1 EC_{50}. As both **32** and **33** provide adequate exposure in CNS, they are both excellent candidates for animal efficacy models of toxoplasmosis.

Selectivity Profiling of 32 and 33

Due to the impressive PK properties of **32** and **33**, these inhibitors were profiled further. To demonstrate that TgCDPK1 is the kinase target of these compounds in *T. gondii*, compounds **32** and **33** were tested against parasitic cell lines overexpressing the Gly128Met TgCDPK1 gatekeeper mutant or wildtype (wt) TgCDPK1. Expression of the Gly128Met gatekeeper mutant of TgCDPK1, but not wt TgCDPK1, makes *T. gondii* highly resistant to PP-based inhibitors that contain 6-alkoxynaphthalen-2-yl groups at the R_1 position.[19,33] Both **32** and **33** show a dramatic loss in potency against parasites overexpressing the Gly128Met gatekeeper mutant relative to the parent RH strain and to *T. gondii* overexpressing wild type TgCDPK1 (Figure 5), which is consistent with TgCDPK1 being the primary target through which these inhibitors exert their anti-parasitic effects.

32 and **33** were further profiled for any mammalian kinase off targets using a panel of 80 human kinases representing different subfamilies of the kinome tree with a fluorescence-based competition assay (Supporting Information Table 1).[17] 78 of the 80 mammalian kinases tested have an $IC_{50} >1.5$ μM (>1500-fold selective for TgCDPK1) for **32**. For the two kinases–PKCν (PKD3) and MEK1–that have sub-micromolar IC_{50} values, compound **32** is a >120-fold and >900-fold less potent inhibitor than for TgCDPK1, respectively. Compound **33** appears to be slightly more selective than compound **32**. Indeed, it demonstrated an IC_{50} value of greater than 5 μM (>2500-fold selective) for 79 of the kinases tested, with only PKCν (PKD3) demonstrating a sub-micromolar ($IC_{50} = 0.280$ μM; 140-fold selective) IC_{50} value.

Structure of the *Tg*CDPK1·33 Complex

Previously, we demonstrated that certain substituents at the R_2 position of the pyrazolopyrimidine scaffold enhance inhibitor potency and selectivity for *Tg*CDPK1.[25] While **1** has an IC_{50} of 2.9 nM for *Tg*CDPK1 and is >3000-fold selective for *Tg*CDPK1 over the mammalian tyrosine kinase Src, the R_2 isopropyl analog of **1** has an IC_{50} of 5.0 nM for *Tg*CDPK1 and is only 76-fold selective for *Tg*CDPK1 over Src.[19,25] The 2-methylpropan-2-ol R_2 group of inhibitors **32** and **33** seem to have a similar effect on selectivity as the *N*-methyl-4-piperidinemethylene group of **1**. For example, the R_2 isopropyl analog of inhibitor **33** is only 40–fold selective for *Tg*CDPK1 over Src, while **33**, which contains a 2-methylpropan-2-ol R_2 group, is >5000-fold selective. To gain a better understanding of the contribution of the 2-methylpropan-2-ol R_2 group to inhibitor binding, a co-crystal structure of **33** bound to *Tg*CDPK1 in the calcium-free inactive form was determined (Figure 6). As expected, **33** occupies the ATP-binding cleft of *Tg*CDPK1, with the pyrazolopyrimidine scaffold making the same hydrophobic and hydrogen-bonding contacts as the adenine ring of ATP. In addition, the 2-cyclopropyloxyquinolin-6-yl R_1 group of **33** is directed towards the Gly128 gatekeeper residue of *Tg*CDPK1, with the quinoline moiety occupying the enlarged hydrophobic pocket that is available due to the lack of a side chain at this position. Side chains of residues in helix-αC and the fourth β-strand of the *N*-terminal lobe form hydrophobic interactions with the 2-cyclopropyloxy group, most likely contributing to the favorable potencies of inhibitors containing this substituent. The R_2 substituent of **33** occupies the ribose-binding pocket of *Tg*CDPK1, with the tertiary alcohol of the R_2 substituent directed towards the phosphate-binding loop (P-loop), which caps the ATP-binding site. Superposition of the *Tg*CDPK1·**33** complex with the co-crystal structure of *Tg*CDPK1 bound to a close analog of **1** shows that the pyrazolopyrimidine scaffolds and R_1 substituents of these inhibitors are well aligned within the ATP-binding site. However, the R_2 groups of both inhibitors adopt very different orientations. While the 2-methylpropan-2-ol R_2 group of **33** is oriented towards the P-loop of *Tg*CDPK1, the larger 4-piperidinemethylene group of the **1** analog is directed out of the ATP-binding site (Figure 6C) and forms an electrostatic interaction with the side chain of Glu155, located on the surface of the C-terminal lobe. Therefore, it appears that different interactions in the ribose pocket can be exploited by R_2 substituents to confer high selectivity for *Tg*CDPK1.

Large Animal Pharmacokinetics

The lack of toxicity in the initial mouse toxicity screens allowed us to move forward into large animal pharmacokinetic and tolerability profiling. Male calves (n=2 for each compound) were dosed orally at 10 mg/kg for compound **32** and 9.3 mg/kg for compound **33** and blood sampled up to 12 days after dosing (Figure 7). Similar to rats, the absorption of both compounds was slow with maximum concentrations reached at 24 hours for compound **33** and 12 hours for compound **32**. The maximum plasma concentrations were similar for the two compounds, 7.9 µM and 9.8 µM for compound **32** and **33**, respectively. However, the overall exposure to **33** was greater than that of **32** due to its lower oral clearance and longer half-life (Table 6). Yet, both compounds had very low oral clearances and long systemic half-lives. Similar to rats, compound **33** had a higher apparent volume of distribution than

compound **32** and the overall distribution characteristics were similar to those observed in rats.

There were some notable calf health concerns following the single oral dose of compound **33**. For compound **33**, both calves developed neurologic signs of toxicity on day 4–5 post-dose. Both calves were observed to have a plantigrade stance and ataxia. Despite abnormalities, both calves were ambulatory, alert, and responsive with normal appetites. The signs became progressively worse, with notable ataxia, followed by marked improvement by day 10 but were never completely resolved by the end of the experiment on day 14. These signs were not observed for compound **32**. One possibility for the increased CNS toxicity was the greater brain exposure for compound **33** compared with compound **32**. The observed neurological signs of toxicity in compound **33** gave us reasons to no longer pursue further studies of this compound. Moving forward we chose to further characterize compound **32** before performing small animal efficacy studies and large animal PK studies.

Further Toxicity Profiling of 32

Potential further toxicity of compound **32** was examined in mice by testing two doses (30 mg/kg and 100 mg/kg PO) daily for five days, while observing mice for signs of toxicity and collecting blood samples. Both groups of mice remained active, well-groomed, and appeared normal throughout the study. Upon necropsy, there were no gross abnormalities. Histology revealed mild focal inflammation in the spleen in two of three mice in the 30 mg/kg group. The only abnormality seen in the 100 mg/kg group was inflammatory infiltrate in the hepatic lobules in one of three mice. The concentrations following 30 mg/kg doses were slightly higher than those predicted from single dose PK data while the exposures following the 100 mg/kg doses were similar to those predicted from single 10 mg/kg dose data (Figure 8). Similar to the early multiple dosing experiments in mice, after the last 100 mg/kg dose the elimination of compound **32** was slower than predicted with considerable plasma concentrations persisting at 72 hours after the final dose.

Next, we completed a maximally tolerated dose study to determine the lowest observable adverse effect level (LOAEL) and the no observable adverse effect level (NOAEL) of compound **32**. Mice were dosed with single PO doses of **32** ranging from 200 mg/kg to 1000 mg/kg. The LOAEL was observed at 500 mg/kg and the NOAEL was observed at 400 mg/kg. Mice had slightly ruffled fur and were less active than the control mice at 3 hours following the 500 mg/kg dose. The lowered activity persisted at 24 hours but was resolved by 30 hours. The lack of toxicity up to 500 mg/kg confirmed the safety of the compound for small animal efficacy studies.

Large Animal Pharmacokinetics of 32

The pharmacokinetics of **32** was further explored in dogs and monkeys following IV and PO administration. Similar to rats, **32** had a very low clearance in both species and a relatively long half-life (Table 7). The plasma concentrations time-profile following IV dosing was biphasic in both species with a similar extent of distribution in dogs and monkeys as observed in rats and calves (Figure 9). The bioavailability of compound **32** was 66 ±17% in

monkeys and 88 ±12% in dogs demonstrating good bioavailability in both species as predicted from rats.

In Vivo Efficacy of 32 Against Acute and Latent *T. gondii* Infection in Mice

We tested **32** against a high inoculum of type I RH strain *T. gondii* to determine efficacy against fulminate toxoplasmosis in two experiments (Figure 10). Unlike type II *T. gondii* strains, type I strains do not typically form tissue cysts but rather cause death within 10 days. Compound **32** was administered *via* oral gavage two days after infection and the burden of infection was measured 5 days after the initiation of treatment. Treatment with **32** at 20 mg/kg for 5 days reduced the number of *T. gondii* tachyzoites in the peritoneal fluid below the limits of detection (less than 100 tachyzoites/mL). Treatment with **32** was highly effective at 20 mg/kg daily for 5 days in reducing infection in the spleen (more than 99%), and infection in the brain (95%). The efficacy of **32** against an acute *T. gondii* infection that is not adequately controlled by the mouse immune system suggests that **32** would be active against toxoplasmosis in an immunocompromised human.

We next tested **32** for its efficacy against latent murine toxoplasmosis by determining its ability to reduce *T. gondii* brain cysts (Fig. 11).[34] Mice were infected IP with the type II ME49 strain of *T. gondii*, which recapitulates the non-lethal course of infection seen in humans, culminating in formation of cysts in the brain. Five weeks after infection, mice were treated once daily for 14 days *via* oral gavage with either 30 mg/kg of **32** or a vehicle control. An additional group of mice was dosed twice–days 1 and 7–with 105 mg/kg of **32**. Mice were sacrificed and cyst numbers were determined from brain homogenate by microscopy two weeks after the last drug dose. The mean number of brain cysts for vehicle-treated control mice was 1537 ±623. Treatment with 30 mg/kg of **32** led to a reduction of brain cyst number of 88.7%. The percent reduction in brain cyst number for the 105 mg/kg-treated group was essentially the same (87.6%). Importantly, no signs of toxicity or increased morbidity were observed in either drug-treated group. The favorable safety profile and brain permeability of **32** make it an attractive candidate to treat toxoplasmosis in pregnancy, as well as CNS toxoplasmosis, although we have not fully investigated it for effects on fetal development.

Conclusions

In the present study, we sought to identify PP-based inhibitors that possess all of the favorable properties of lead compound **1** but lack its hERG activity. To do this, analogs of **1**, which contain variable R_1 and R_2 groups displayed from the PP-scaffold, were first screened for potent inhibition of the *Tg*CDPK1 enzyme and *T. gondii* invasion/proliferation. Inhibitors of sufficient potency were then screened for the lack of growth inhibition of mammalian cell lines and minimal hERG activity. In this series of inhibitors, the key to eliminating hERG activity was replacing the *N*-methyl-4-piperidinemethylene R_2 position group of **1** with a non-basic substituent that is able to confer a similar level of *Tg*CDPK1 selectivity. While a number of non-basic R_2 substituents provided inhibitors with potent activity against *T. gondii* and minimal mammalian cell cytotoxicity and hERG activity, inhibitors **32** and **33**, which contain a 2, 2-dimethylpropan-1-ol group at the R_2 position,

stood out due to their superior PK properties and adequate exposure to the CNS. However, the superior safety profile of inhibitor **32** coupled with its favorable pharmacokinetic characteristics in small and large animals made this compound the focus of anti-toxoplasmosis efficacy studies. The efficacy of **32** in mouse models of acute and latent toxoplasmosis points to the promise of this drug for further development.

EXPERIMENTAL PROCEDURES

General Synthetic Methods

All chemicals were purchased from commercial suppliers and used without further purification unless otherwise stated. Reactions were monitored with thin-layer chromatography using silica gel 60 F254 coated glass plates (EM Sciences). Compound purification was performed with an IntelliFlash 280 automated flash chromatography system/Combi flash Rf+ using pre-packed Varian Super Flash/Redi sep Rf silica gel columns (hexanes/EtOAc or CH_2Cl_2/MeOH gradient solvent systems). A Varian Dynamax Microsorb 100-5 C_{18} column (250 mm × 21.4 mm), eluting with H_2O/CH_3CN and H_2O/MeOH gradient solvent systems (+0.05% TFA) was used for preparatory HPLC purification. Products were detected by UV at λ=254 & 220 nm. The purity of all final compounds was determined by two analytical RP-HPLC methods, using an Agilent ZORBAX SB-C_{18} (2.1 mm × 150 mm) or Varian Microsorb-MV 100-5 C_{18} column (4.6 mm × 150 mm), and eluting with either H_2O/CH_3CN or H_2O/MeOH gradient solvent systems (+0.05% TFA) run over 30 min. Products were detected by UV at λ=254 nm, with all final compounds displaying >95% purity. NMR spectra were recorded on Bruker 300 or 500 MHz spectrometers at ambient temperature. Chemical shifts are reported in parts per million (δ) and coupling constants in Hz. ^{1}H-NMR spectra were referenced to the residual solvent peaks as internal standards (7.26 ppm for $CDCl_3$, 2.50 ppm for d_6-DMSO, and 3.34 ppm for CD_3OD). Mass spectra were recorded with a Bruker Esquire Liquid Chromatograph - Ion Trap Mass Spectrometer. The synthetic routes used to generate inhibitors are shown in Schemes 1–3.

Synthesis and purification methods for compounds **1–9** in Table 1 are described in previous publications.[19,26] Protocols for synthesis of intermediates are provided in the Supporting Information.

General R_2 alkylation procedure—Pyrazolopyrimidine (1 equiv.), K_2CO_3 or Cs_2CO_3 or K_2CO_3:NaH_2PO_4 (1.5–2 equiv.), and an alkylhalide (1.1 equiv.) or alkylmesylate (1.1 equiv.) or oxirane (1.1 equiv.) were stirred in dry DMF at room temperature or 80 °C. The reaction was monitored by thin layer chromatography. After completion, ethyl acetate and water were added and the organic phase was separated. The water phase was extracted with ethyl acetate. The combined organic phases were washed with brine, dried over Na_2SO_4 and evaporated under reduced pressure. The crude product was then purified *via* flash chromatography over silica, eluting with either a hexanes/EtOAc or CH_2Cl_2/MeOH gradient. If necessary, further purification was performed with preparatory RP-HPLC.

General Suzuki coupling procedure—3-Iodopyrazolopyrimidines or 3-Bromopyrazolopyrimidines (1 equiv.), Na_2CO_3 or K_3PO_4 (2–4 equiv.), Pd(PPh$_3$)$_4$ or

Pd(II)Cl$_2$dppf.DCM, (0.05 equiv.) and boronic acids or boronate pinacol esters (1–2 equiv.) were dissolved in a mixture of dimethoxyethane (1.5 mL) and water (0.5 mL) and then heated in a microwave at 80 °C for one hour. The reaction was monitored by thin layer chromatography. After cooling, ethyl acetate and water were added and the organic phase was separated. The water phase was extracted with ethyl acetate. The combined organic phases were washed with brine, dried over Na$_2$SO$_4$ and evaporated under reduced pressure. The crude product was then purified *via* flash chromatography over silica, eluting with either a hexanes/EtOAc or CH$_2$Cl$_2$/MeOH gradient. If necessary, further purification was performed with preparatory RP-HPLC.

General naphthol alkylation procedure—6-Hydroxy-2-naphthalene pyrazolopyrimidines (1 equiv.), K$_2$CO$_3$ or Cs$_2$CO$_3$ (1.5–2 equiv.), and alkyl halides/epoxides (1.1 equiv.), NaH$_2$PO$_4$:K$_2$CO$_3$ (1:1 equiv.), were stirred in dry DMF at room temperature or 60–80 °C and monitored by thin layer chromatography. After completion, ethyl acetate and water were added and the organic phase was separated. The water phase was extracted with ethyl acetate. The combined organic phases were washed with brine, dried over Na$_2$SO$_4$, and evaporated under reduced pressure. The crude product was then purified *via* flash chromatography over silica, eluting with either a hexanes/EtOAc or CH$_2$Cl$_2$/MeOH gradient. If necessary, further purification was performed with preparatory RP-HPLC.

General boc-deprotection procedure—Boc-amine-containing pyrazolopyrimidine was stirred in a TFA/CH$_2$Cl$_2$ (1:1) mixture for ~3 h. The reaction was then concentrated and purified *via* preparatory RP-HPLC. After HPLC purification, the product was then re-concentrated from 1.25 M HCl in EtOH to afford the final, purified product as a bis-HCl salt.

General reductive amination procedure—Deprotected pyrazolopyrimidines (1 equiv.) were dissolved in methanol and neutralized with sodium methoxide. A solution containing 2% acetic acid and an aldehyde or ketone (5–10 equiv.) was stirred at room temperature for 10 min. Sodium cyanoborohydride (5 equiv.) was then added and the reaction was stirred until reaching completion, as determined by thin layer chromatography (typically ~2 h). The crude reaction was then purified *via* preparatory RP-HPLC. After HPLC purification, the residue was dissolved in a small amount of 2 M HCl in methanol and, after concentration *in vacuo*, the final product was obtained as an HCl salt.

3-(6-(Cyclopropylmethoxy)naphthalen-2-yl)-1-((1-methylpiperidin-4-yl)methyl)-1H-pyrazolo[3,4-d]pyrimidin-4-amine (10): *Tert*-butyl-4-((4-amino-3-(6-hydroxynaphthalen-2-yl)-1*H*-pyrazolo[3,4-*d*]pyrimidin-1-yl)methyl)piperidine-1-carboxylate[26] and (bromomethyl)cyclopropane were subjected to the ***General naphthol alkylation procedure*** followed by the ***General boc-deprotection procedure*** and ***General reductive amination procedure*** in order to afford **10**. ^{1}H NMR (300 MHz, CD$_3$OD) δ 8.51 (s, 1H), 8.17 (s, 1H), 8.01 (d, *J* = 8.5 Hz, 1H), 7.93 (d, *J* = 9.1 Hz, 1H), 7.81 (d, *J* = 9.3 Hz, 1H), 7.36 (s, 1H), 7.30 (d, *J* = 9.3 Hz, 1H), 4.56 (d, *J* = 6.4 Hz, 2H), 4.03 (d, *J* = 6.6 Hz, 2H), 3.57 (m, 2H), 3.06 (m, 2H), 2.88 (s, 3H), 2.45 (m, 1H), 2.02 (m, 2H), 1.77 (m, 2H), 1.44 (m, 1H), 0.71 (m, 2H), 0.46 (m, 2H); MS (ESI) 443.5 *m/z* [MH+], C$_{26}$H$_{31}$N$_6$O requires 443.5.

3-(6-Cyclobutoxynaphthalen-2-yl)-1-((1-methylpiperidin-4-yl)methyl)-1H-pyrazolo[3,4-d]pyrimidin-4-amine (11): 2-(6-Cyclobutoxynaphthalen-2-yl)-4,4,5,5-tetramethyl-1,3,2-dioxaborolane (**38**) and *tert*-butyl-4-((4-amino-3-iodo-1*H*-pyrazolo[3,4-*d*]pyrimidin-1-yl)methyl)piperidine-1-carboxylate[19] were subjected to the ***General Suzuki coupling procedure*** followed by the ***General boc-deprotection procedure*** and ***General reductive amination procedure*** in order to afford **11**. ^{1}H NMR (300 MHz, CD$_3$OD) δ 8.47 (s, 1H), 8.15 (s, 1H), 7.99 (d, *J* = 8.3 Hz, 1H), 7.92 (d, *J* = 9.5 Hz, 1H), 7.80 (d, *J* = 8.9 Hz, 1H), 7.24 (m, 2H), 4.53 (d, *J* = 6.6 Hz, 2H), 3.56 (m, 2H), 3.03 (m, 2H), 2.86 (s, 3H), 2.62 (m, 2H), 2.44 (m, 1H), 2.22 (m, 2H), 2.04–1.60 (m, 6H); MS (ESI) 443.4 *m/z* [MH+], C$_{26}$H$_{31}$N$_6$O requires 443.2.

3-(6-Cyclopropoxynaphthalen-2-yl)-1-((1-methylpiperidin-4-yl)methyl)-1H-pyrazolo[3,4-d]pyrimidin-4-amine (12): 2-(6-Cyclopropoxynaphthalen-2-yl)-4,4,5,5-tetramethyl-1,3,2- dioxaborolane (**41**) and *tert*-butyl-4-((4-amino-3-iodo-1*H*-pyrazolo[3,4-*d*]pyrimidin-1-yl)methyl)piperidine-1-carboxylate were subjected to the ***General Suzuki coupling procedure*** followed by the ***General boc-deprotection procedure*** and ***General reductive amination procedure*** in order to afford **12**. ^{1}H NMR (300 MHz, CD$_3$OD) δ 8.49 (s, 1H), 8.17 (s, 1H), 8.03 (d, *J* = 8.5 Hz, 1H), 7.92 (d, *J* = 9.1 Hz, 1H), 7.80 (d, *J* = 8.5 Hz, 1H), 7.64 (d, *J* = 2.0 Hz, 1H), 7.27 (dd, *J* = 8.9, 1.8 Hz, 1H), 4.52 (d, *J* = 6.0 Hz, 2H), 3.98 (m, 1H), 3.56 (m, 2H), 3.05 (m, 2H), 2.87 (s, 3H), 2.44 (m, 1H), 2.00 (m, 2H), 1.76 (m, 2H), 0.92 (m, 2H), 0.80 (m, 2H); MS (ESI) 429.5 *m/z* [MH+], C$_{25}$H$_{29}$N$_6$O requires 429.6.

3-(6-(2-Methoxyethoxy)naphthalen-2-yl)-1-((1-methylpiperidin-4-yl)methyl)-1H-pyrazolo[3,4-d]pyrimidin-4-amine (13): *Tert*-butyl-4-((4-amino-3-(6-hydroxynaphthalen-2-yl)-1*H*-pyrazolo[3,4-*d*]pyrimidin-1-yl)methyl)piperidine-1-carboxylate[26] and bromomethoxyethane were subjected to the ***General naphthol alkylation procedure*** followed by the ***General boc-deprotection procedure*** and ***General reductive amination procedure*** in order to afford **13**. ^{1}H NMR (300 MHz, CD$_3$OD) δ 8.50 (s, 1H), 8.16 (s, 1H), 8.01 (d, *J* = 7.8 Hz, 1H), 7.93 (d, *J* = 8.5 Hz, 1H), 7.80 (d, *J* = 8.3 Hz, 1H), 7.40 (s, 1H), 7.30 (d, *J* = 7.8 Hz, 1H), 4.52 (d, *J* = 4.2 Hz, 2H), 4.31 (m, 2H), 3.86 (m, 2H), 3.62 (m, 2H), 3.54 (s, 3H), 3.04 (m, 2H), 2.87 (s, 3H), 2.44 (m, 1H), 1.99 (m, 2H), 1.77(m, 2H); MS (ESI) 447.5 *m/z* [MH+], C$_{25}$H$_{31}$N$_6$O$_2$ requires 447.5.

1-((1-Methylpiperidin-4-yl)methyl)-3-(6-(oxetan-3-yloxy)naphthalen-2-yl)-1H-pyrazolo[3,4-d]pyrimidin-4-amine (14): *Tert*-butyl-4-((4-amino-3-(6-hydroxynaphthalen-2-yl)-1*H*-pyrazolo[3,4-*d*]pyrimidin-1-yl)methyl)piperidine-1-carboxylate[19] and 3-bromooxetane were subjected to the ***General naphthol alkylation procedure*** followed by the ***General boc-deprotection procedure*** and ***General reductive amination procedure*** in order to afford **14**. ^{1}H NMR (300 MHz, CD$_3$OD) δ 8.49 (s, 1H), 8.18 (s, 1H), 8.06–7.92 (m, 2H), 7.82 (d, *J* = 8.5 Hz, 1H), 7.51 (s, 1H), 7.36 (d, *J* = 9.1 Hz, 1H), 4.81 (m, 1H), 4.53 (d, *J* = 5.6 Hz, 2H), 3.99–3.84 (m, 4H), 3.57 (m, 2H), 3.05 (m, 2H), 2.86 (s, 3H), 2.44 (m, 1H), 2.00 (m, 2H), 1.74 (m, 2H); MS (ESI) 445.2 *m/z* [MH+], C$_{25}$H$_{29}$N$_6$O$_2$ requires 445.2.

2-(6-(4-Amino-1-((1-methylpiperidin-4-yl)methyl)-1H-pyrazolo[3,4-d]pyrimidin-3-yl)naphthalen-2-yloxy)ethanol (15): *Tert*-butyl-4-((4-amino-3-(6-hydroxynaphthalen-2-yl)-1*H*-pyrazolo[3,4-*d*]pyrimidin-1-yl)methyl)piperidine-1-carboxylate[19] and oxirane were subjected to the ***General naphthol alkylation procedure*** followed by the ***General boc-deprotection procedure*** and ***General reductive amination procedure*** in order to afford **15**. ^{1}H NMR (300 MHz, CD$_3$OD) δ 8.50 (s, 1H), 8.17 (s, 1H), 8.02 (d, J = 8.3 Hz, 1H), 7.94 (d, J = 8.9 Hz, 1H), 7.80 (d, J = 8.9 Hz, 1H), 7.41 (d, J = 2.2 Hz, 1H), 7.34 (dd, J = 8.7, 2.0 Hz, 1H), 4.53 (d, J = 6.4 Hz, 2H), 4.25 (t, J = 4.5 Hz, 2H), 3.99 (t, J = 4.5 Hz, 2H), 3.56 (m, 2H), 3.04 (m, 2H), 2.86 (s, 3H), 2.44 (m, 1H), 2.00 (m, 2H), 1.72 (m, 2H); MS (ESI) 433.3 *m/z* [MH+], C$_{24}$H$_{29}$N$_6$O$_2$ requires 433.5.

1-(6-(4-Amino-1-((1-methylpiperidin-4-yl)methyl)-1H-pyrazolo[3,4-d]pyrimidin-3-yl)naphthalen-2-yloxy)-2-methylpropan-2-ol (16): *Tert*-butyl-4-((4-amino-3-(6-hydroxynaphthalen-2-yl)-1*H*-pyrazolo[3,4-*d*]pyrimidin-1-yl)methyl)piperidine-1-carboxylate[19] and 2,2-dimethyloxirane were subjected to the ***General naphthol alkylation procedure*** followed by the ***General boc-deprotection procedure*** and ***General reductive amination procedure*** in order to afford **16**. ^{1}H NMR (300 MHz, CD$_3$OD) δ 8.48 (s, 1H), 8.17 (s, 1H), 8.02 (d, J = 8.9 Hz, 1H), 7.94 (d, J = 8.7 Hz, 1H), 7.79 (d, J = 8.5 Hz, 1H), 7.43–7.32 (m, 2H), 4.53 (d, J = 6.8 Hz, 2H), 3.98 (s, 2H), 3.56 (m, 2H), 3.04 (m, 2H), 2.87 (s, 3H), 2.44 (m, 1H), 2.00 (m, 2H), 1.77 (m, 2H), 1.41 (s, 6H); MS (ESI) 461.5 *m/z* [MH+], C$_{26}$H$_{33}$N$_6$O$_2$ requires 461.5.

3-(2-Ethoxyquinolin-6-yl)-1-((1-methylpiperidin-4-yl)methyl)-1H-pyrazolo[3,4-d]pyrimidin-4-amine (17): *Tert*-butyl-4-((4-amino-3-(2-ethoxyquinolin-6-yl)-1*H*-pyrazolo[3,4-*d*]pyrimidin-1-yl)methyl)piperidine-1-carboxylate[26] was subjected to the ***General boc-deprotection procedure*** and ***General reductive amination procedure*** in order to afford **17**. ^{1}H NMR (300 MHz, CD$_3$OD) δ 8.29 (s, 1H), 8.22 (d, J = 8.2 Hz, 1H), 8.12 (s, 1H), 7.98 (m, 2H), 7.04 (d, J = 8.5 Hz, 1H), 4.55 (q, J = 6.8 Hz, 2H), 4.38 (d, J = 4.3 Hz, 2H), 2.95 (m, 2H), 2.30 (s, 3H), 2.99 (m, 2H), 1.67 (m, 2H), 1.48 (m, 4H); MS (ESI) 418.3 *m/z* [MH+], C$_{23}$H$_{28}$N$_7$O requires 418.5.

1-((1-Methylpiperidin-4-yl)methyl)-3-(2-(2,2,2-trifluoroethoxy)quinolin-6-yl)-1H-pyrazolo[3,4-d]pyrimidin-4-amine (18): 2-(2,2,2-Trifluoroethoxy)quinolin-6-ylboronic acid (**39**) and *tert*-butyl-4-((4-amino-3-iodo-1*H*-pyrazolo[3,4-*d*]pyrimidin-1-yl)methyl)piperidine-1-carboxylate[19] were subjected to the ***General Suzuki coupling procedure*** followed by the ***General boc-deprotection procedure*** and ***General reductive amination procedure*** in order to afford **18**. ^{1}H NMR (300 MHz, CD$_3$OD) δ 8.49 (s, 1H), 8.39 (d, J = 8.5 Hz, 1H), 8.24 (s, 1H), 8.04 (s, 2H), 7.18 (d, J = 7.0 Hz, 1H), 5.09 (q, J = 8.7 Hz, 2H), 4.52 (s, 2H), 3.54 (m, 2H), 3.04 (m, 2H), 2.84 (s, 3H), 2.45 (m, 1H), 1.98 (m, 2H), 1.75 (m, 2H); MS (ESI) 472.2 *m/z* [MH+], C$_{23}$H$_{25}$F$_3$N$_7$O requires 472.5.

3-(2-Cyclopropoxyquinolin-6-yl)-1-((1-methylpiperidin-4-yl)methyl)-1H-pyrazolo[3,4-d]pyrimidin-4-amine (19): 2-Cyclopropoxyquinolin-6-ylboronic acid (**40**) and *tert*-butyl-4-((4-amino-3-iodo-1*H*-pyrazolo[3,4-*d*]pyrimidin-1-yl)methyl)piperidine-1-carboxylate[19] were subjected to the ***General Suzuki coupling procedure*** followed by the ***General boc-***

deprotection procedure and *General reductive amination procedure* in order to afford
19. ^{1}H NMR (300 MHz, CD$_3$OD) δ 9.17 (s, 1H), 8.75–8.33 (m, 3H), 8.28–7.98 (m, 2H),
4.72 (m, 1H), 4.54 (d, J = 6.0 Hz, 2H), 3.56 (m, 2H), 3.10 (m, 2H), 3.00 (s, 3H), 2.48 (m,
1H), 2.00 (m, 2H), 1.60 (m, 2H), 1.20–1.10 (m, 4H); MS (ESI) 430.5 *m/z* [MH+],
C$_{24}$H$_{28}$N$_7$O requires 430.6.

3-(2-Cyclopropoxyquinolin-6-yl)-1-(3-(dimethylamino)-2,2-dimethylpropyl)-1H-pyrazolo[3,4-d]pyrimidin-4-amine (20): 2-Cyclopropoxyquinolin-6-ylboronic acid (**40**)
and 1-(3-(dimethylamino)-2,2-dimethylpropyl)-3-iodo-1*H*-pyrazolo[3,4-*d*]pyrimidin-4-
amine (**42**) were subjected to the *General Suzuki coupling procedure* to afford **20**. ^{1}H NMR
(300 MHz, CD$_3$OD) δ 8.29 (s, 1H), 8.22 (d, J = 8.9 Hz, 1H,), 8.11 (d, J = 1.6 Hz, 1H) 8.01
(s, 1H), 8.00 (dd, J = 8.5, 1.5 Hz, 1H,), 7.07 (d, J = 8.9 Hz, 1H), 4.46 (m, 1H), 4.36 (s, 2H),
2.46 (s, 2H), 2.44 (s, 6H), 1.03 (s, 6H), 0.93–0.82 (m, 4H). MS (ESI) 432.6 *m/z* [MH+],
C$_{24}$H$_{30}$N$_7$O requires 432.5.

3-(6-Ethoxynaphthalen-2-yl)-1-isobutyl-1H-pyrazolo[3,4-d]pyrimidin-4-amine (21): 6-
Ethoxynaphthalen-2-ylboronic acid and 3-iodo-1-isobutyl-1*H*-pyrazolo[3,4-*d*]pyrimidin-4-
amine[26] were subjected to the *General Suzuki coupling procedure* in order to afford **21**. [1]H
NMR (300 MHz, CD$_3$OD) δ 8.27 (s, 1H), 8.09 (s, 1H), 7.96 (d, J = 8.1 Hz, 1H), 7.89 (d, J =
9.1 Hz, 1H), 7.75 (dd, J = 8.2, 2.0 Hz, 1H), 7.32 (s, 1H), 7.22 (dd, J = 9.1, 2.4 Hz, 1H),
4.28–4.17 (m, 4H), 2.39 (m, 1H), 1.48 (t, J = 6.8 Hz, 3H), 0.96 (d, J = 6.6 Hz, 6H); MS
(ESI) 362.4 *m/z* [MH+], C$_{21}$H$_{24}$N$_5$O requires 362.2.

**3-(6-Cyclopropoxynaphthalen-2-yl)-1-isobutyl-1H-pyrazolo[3,4-d]pyrimidin-4-amine
(22):** 6-(4-Amino-1-isobutyl-1*H*-pyrazolo[3,4-*d*]pyrimidin-3-yl)naphthalen-2-ol (**46**) and
bromocyclopropane were subjected to the *General naphthol alkylation procedure* in order
to afford **22**. ^{1}H NMR (300 MHz, CD$_3$OD) δ 8.27 (s, 1H), 8.10 (s, 1H), 7.98 (d, J = 8.7 Hz,
1H), 7.89 (d, J = 8.9 Hz, 1H), 7.76 (dd, J = 8.5, 1.6 Hz, 1H), 7.61 (d, J = 2.2 Hz, 1H), 7.25–
7.18 (dd, J = 8.9, 2.2 Hz, 1H), 4.24 (d, J = 7.25 Hz, 2H), 3.95 (m, 1H), 2.38 (m, 1H), 0.97 (d,
J = 6.6 Hz, 6H), 0.90 (m, 2H), 0.79 (m, 2H); MS (ESI) 374.2 *m/z* [MH+], C$_{22}$H$_{24}$N$_5$O
requires 374.4.

**3-(2-Cyclopropoxyquinolin-6-yl)-1-isobutyl-1H-pyrazolo[3,4-d]pyrimidin-4-amine
(23):** 2-Cyclopropoxyquinolin-6-ylboronic acid (**40**) and 3-iodo-1-isobutyl-1*H*-pyrazolo[3,4-
d]pyrimidin-4-amine[26] were subjected to the *General Suzuki coupling procedure* in order
to afford **23**. ^{1}H NMR (300 MHz, CD$_3$OD) δ 8.25 (s, 1H), 8.23 (d, J = 8.9 Hz, 1H), 8.10 (s,
1H), 8.00–7.91 (m, 2H), 7.02 (d, J = 8.7 Hz, 1H), 4.46 (s, 1H), 4.22 (d, J = 7.4 Hz, 2H), 2.36
(m, 1H), 0.96 (d, J = 6.6 Hz, 6H), 0.91–0.72 (m, 4H); MS (ESI) 375.4 *m/z* [MH+],
C$_{21}$H$_{23}$N$_6$O requires 375.4.

3-(6-Cyclopropoxynaphthalen-2-yl)-1-((3-methyloxetan-3-yl)methyl)-1H-pyrazolo[3,4-d]pyrimidin-4-amine (24): 2-(6-Cyclopropoxynaphthalen-2-yl)-4,4,5,5-tetramethyl-1,3,2-
dioxaborolane (**41**) and 3-iodo-1-((3-methyloxetan-3-yl)methyl)-1*H*-pyrazolo[3,4-
d]pyrimidin-4-amine (**44**) were subjected to the *General Suzuki coupling procedure* in
order to afford **24**. ^{1}H NMR (300 MHz, CDCl$_3$) δ 8.39 (s, 1H), 8.08 (s, 1H), 7.93 (d, J = 8.7

Hz, 1H), 7.83 (d, *J* = 8.9 Hz, 1H), 7.77 (d, *J* = 9.4 Hz, 1H), 7.52 (s, 1H), 7.24 (dd, *J* = 10.0, 3.0 Hz, 1H), 5.68 (s, 2H), 4.90 (d, *J* = 6.1 Hz, 2H), 4.64 (s, 2H), 4.45 (d, *J* = 6.1 Hz, 2H), 3.91 (m, 1H), 1.36 (3, 3H), 0.96–0.83 (m, 4H); MS (ESI) 402.2 *m/z* [MH+], $C_{23}H_{24}N_5O_2$ requires 402.4.

3-(2-Cyclopropoxyquinolin-6-yl)-1-((3-methyloxetan-3-yl)methyl)-1H-pyrazolo[3,4-d]pyrimidin-4-amine (25): 2-Cyclopropoxyquinolin-6-ylboronic acid (**40**) and 3-iodo-1-((3-methyloxetan-3-yl)methyl)-1*H*-pyrazolo[3,4-*d*]pyrimidin-4-amine (**44**) were subjected to the *General Suzuki coupling procedure* in order to afford **25**. ^{1}H NMR (300 MHz, CDCl₃) δ 8.41 (s, 1H), 8.12–8.01 (m, 3H), 7.96 (d, *J* = 8.3 Hz, 1H), 6.97 (d, *J* = 8.0 Hz, 1H), 5.54 (s, 2H), 4.91 (d, *J* = 6.1 Hz, 2H), 4.64 (s, 2H), 4.56 (m, 1H), 4.45 (d, *J* = 6.1 Hz, 2H), 1.36 (s, 3H), 0.95–0.82 (m, 4H); MS (ESI) 403.2 *m/z* [MH+], $C_{22}H_{23}N_6O_2$ requires 403.4.

3-(6-Cyclopropoxynaphthalen-2-yl)-1-((tetrahydro-2H-pyran-4-yl)methyl)-1H-pyrazolo[3,4-d]pyrimidin-4-amine (28): 2-(6-Cyclopropoxynaphthalen-2-yl)-4,4,5,5-tetramethyl-1,3,2-dioxaborolane (**41**) and 3-iodo-1-((tetrahydro-2*H*-pyran-4-yl)methyl)-1*H*-pyrazolo[3,4-*d*]pyrimidin-4-amine[26] were subjected to the *General Suzuki coupling procedure* in order to afford **28**. ^{1}H NMR (300 MHz, CD₃OD) δ 8.47 (s, 1H), 8.16 (s, 1H), 8.03 (d, *J* = 8.2 Hz, 1H), 7.92 (d, *J* = 9.1 Hz, 1H), 7.78 (d, *J* = 8.2 Hz, 1H), 7.64 (s, 1H), 7.27 (dd, *J* = 9.1, 2.2 Hz, 1H) 4.45 (d, *J* = 6.8 Hz, 2H,), 3.99 (m, 1H), 3.76 (m, 2H), 3.05 (m, 2H), 2.40 (m, 1H), 1.61 (m, 2H), 1.46 (m, 2H), 0.93–0.80 (m, 4H); MS (ESI) 416.4 *m/z* [MH+], $C_{24}H_{25}N_5O_2$ requires 416.4.

3-(2-Cyclopropoxyquinolin-6-yl)-1-((tetrahydro-2H-pyran-4-yl)methyl)-1H-pyrazolo[3,4-d]pyrimidin-4-amine (29): 2-Cyclopropoxyquinolin-6-ylboronic acid (**40**) and 3-iodo-1-((tetrahydro-2*H*-pyran-4-yl)methyl)-1*H*-pyrazolo[3,4-*d*]pyrimidin-4-amine[26] were subjected to the *General Suzuki coupling procedure* in order to afford **29**. ^{1}H NMR (300 MHz, CD₃OD) δ 8.31 (s, 1H), 8.22 (d, *J* = 8.9 Hz, 1H), 8.12 (d, *J* = 1.8 Hz, 1H), 8.06 (d, *J* = 8.7 Hz, 1H), 8.00 (dd, *J* = 8.5, 1.2 Hz, 1H), 7.07 (d, *J* = 8.9 Hz, 1H), 4.47 (m, 1H) 4.36 (d, *J* = 7.2 Hz, 2H,), 3.98 (m, 2H), 3.42 (m, 2H), 2.34 (m, 1H), 1.59 (m, 2H), 1.49 (m, 2H), 0.93–0.83 (m, 4H); MS (ESI) 416.4 *m/z* [MH+], $C_{23}H_{24}N_6O_2$ requires 416.4.

1-(4-Amino-3-(6-ethoxynaphthalen-2-yl)-1H-pyrazolo[3,4-d]pyrimidin-1-yl)-2-methylpropan-2-ol (30): 6-Ethoxynaphthalen-2-ylboronic acid (**41**) and 1-(4-amino-3-iodo-1*H*-pyrazolo[3,4-*d*]pyrimidin-1-yl)-2-methylpropan-2-ol (**43**) were subjected to the *General Suzuki coupling procedure* to afford compound **30**; ^{1}H NMR (300 MHz, CD₃OD) δ 8.26 (s, 1H), 8.09 (s, 1H), 7.97–7.83 (m, 2H), 7.76 (dd, *J* = 8.2, 1.4 Hz, 1H), 7.30 (d, *J* = 2.0 Hz, 1H), 7.20 (dd, *J* = 8.9, 1.4 Hz, 1H), 4.41 (s, 2H), 4.19 (q, *J* = 7.0 Hz, 2H), 1.47 (t, *J* = 6.8 Hz, 3H), 1.28 (s, 6H). MS (ESI) 378.2 *m/z* [MH+], $C_{21}H_{24}N_5O_2$ requires 378.1.

1-(4-Amino-3-(2-ethoxyquinolin-6-yl)-1H-pyrazolo[3,4-d]pyrimidin-1-yl)-2-methylpropan-2-ol (31): 2-Ethoxy-6-(4,4,5,5-tetramethyl-1,3,2-dioxaborolan-2-yl)quinoline[19] and 1-(4-amino-3-iodo-1*H*-pyrazolo[3,4-*d*]pyrimidin-1-yl)-2-methylpropan-2-ol (**43**) were subjected to the *General Suzuki coupling procedure* to afford compound **31**; ^{1}H NMR (300 MHz, CD₃OD) δ 8.69 (d, *J* = 9.1 Hz, 1H), 8.45 (s, 1H), 8.34

(s, 1H), 8.17 (d, J = 8.0 Hz, 1H), 8.04 (d, J = 7.4 Hz, 1H), 7.45 (d, J = 7.4 Hz, 1H), 4.67 (q, J = 6.0 Hz, 2H), 4.50 (s, 2H), 1.54 (t, J = 6.5 Hz, 3H), 1.31 (s, 6H). MS (ESI) 379.2 m/z [MH +], $C_{20}H_{23}N_6O_2$ requires 379.1.

1-(4-Amino-3-(6-cyclopropoxynaphthalen-2-yl)-1H-pyrazolo[3,4-d]pyrimidin-1-yl)-2-methylpropan-2-ol (32): 2-(6-Cyclopropoxynaphthalen-2-yl)-4,4,5,5-tetramethyl-1,3,2-dioxaborolane (**41**) and 1-(4-amino-3-iodo-1*H*-pyrazolo[3,4-*d*]pyrimidin-1-yl)-2-methylpropan-2-ol (**43**) were subjected to the *General Suzuki coupling procedure* to afford title compound **32**; ^{1}H NMR (500 MHz, CD3OD) δ 8.26 (s, 1H), 8.08 (s, 1H), 7.93 (d, J = 8.4 Hz, 1H), 7.85 (d, J = 8.81 Hz, 1H), 7.76 (d, J = 8.4 Hz, 1H), 7.57 (s, 1H), 7.20 (dd, J = 8.8, 1.8 Hz, 1H), 4.40 (s, 2H), 3.91 (m, 1H), 1.27 (s, 6H), 0.88 (m, 2H), 0.78 (m, 2H). MS (ESI) 390.2 m/z [MH+], $C_{22}H_{24}N_5O_2$ requires 390.1.

1-(4-Amino-3-(2-cyclopropoxyquinolin-6-yl)-1H-pyrazolo[3,4-d]pyrimidin-1-yl)-2-methylpropan-2-ol (33): 2-Cyclopropoxyquinolin-6-ylboronic acid (**40**) and 1-(4-amino-3-iodo-1*H*-pyrazolo[3,4-*d*]pyrimidin-1-yl)-2-methylpropan-2-ol (**43**) were subjected to the *General Suzuki coupling procedure* in order to afford **33**. NMR (300 MHz, CD3OD) δ 8.28 (s, 1H), 8.28–8.24 (d, J = 8.9 Hz, 1H), 8.15 (t, J = 1.4 Hz, 1H), 8.01 (d, J = 1.2 Hz, 2H), 7.06 (d, J = 8.7 Hz, 1H), 4.53–4.45 (m, 1H), 4.42 (s, 2H), 1.28 (s, 6H), 0.92–0.85 (m, 2H), 0.85–0.77 (m, 2H); MS (ESI) 391.1 m/z [MH[+]], $C_{21}H_{23}N_6O_2$ requires 391.2.

3-(4-Amino-3-(6-cyclopropoxynaphthalen-2-yl)-1H-pyrazolo[3,4-d]pyrimidin-1-yl)-2,2-dimethylpropan-1-ol (34): 2-(6-Cyclopropoxynaphthalen-2-yl)-4,4,5,5-tetramethyl-1,3,2-dioxaborolane (**41**) and previously reported 3-(4-amino-3-iodo-1*H*-pyrazolo[3,4-*d*]pyrimidin-1-yl)-2,2-dimethylpropan-1-ol[26] were subjected to the *General Suzuki coupling procedure* in order to afford **34**. ^{1}H NMR (300 MHz, CD3OD) δ 8.30 (s, 1H), 8.12 (s, 1H), 8.00 (d, J = 8.7 Hz, 1H), 7.90 (d, J = 8.9 Hz, 1H), 7.78 (dd, J = 8.2, 1.5 Hz, 1H), 7.62 (d, J = 2.4, 1H), 7.24 (dd, J = 9.1, 2.4 Hz, 1H), 4.33 (s, 2H), 3.97 (m, 1H), 3.32 (s, 2H), 1.22 (s, 6H), 0.94–0.81 (m, 4H); MS (ESI) 404.5 m/z [MH+], $C_{23}H_{26}N_5O_2$ requires 404.4.

3-(4-Amino-3-(2-cyclopropoxyquinolin-6-yl)-1H-pyrazolo[3,4-d]pyrimidin-1-yl)-2,2-dimethylpropan-1-ol (35): 2-Cyclopropoxyquinolin-6-ylboronic acid (**40**) and previously reported 3-(4-amino-3-iodo-1*H*-pyrazolo[3,4-*d*]pyrimidin-1-yl)-2,2-dimethylpropan-1-ol[26] were subjected to the *General Suzuki coupling procedure* in order to afford **35**. ^{1}H NMR (300 MHz, CD3OD) δ 8.65 (s, 1H), 8.50 (s, 1H), 8.36 (m, 1H), 8.21–8.05 (m, 2H), 7.51 (d, J = 8.3 Hz, 1H), 4.59 (s, 2H), 4.47 (s, 2H), 4.46 (m, 1H), 1.01 (s, 6H), 0.70 (m, 4H); MS (ESI) 405.2 m/z [MH+], $C_{22}H_{25}N_6O_2$ requires 405.4.

3-(4-Amino-3-(2-(2,2,2-trifluoroethoxy)quinolin-6-yl)-1H-pyrazolo[3,4-d]pyrimidin-1-yl)-2,2-dimethylpropan-1-ol (36): 2-(2,2,2-Trifluoroethoxy)quinolin-6-ylboronic acid (**39**) and previously reported 3-(4-amino-3-iodo-1*H*-pyrazolo[3,4-*d*]pyrimidin-1-yl)-2,2-dimethylpropan-1-ol[26] were subjected to the *General Suzuki coupling procedure* in order to afford **36**. ^{1}H NMR (300 MHz, CD3OD) δ 8.40 (s, 1H), 8.17 (d, J = 8.7 Hz, 1H), 8.07 (d, J = 1.6 Hz, 1H), 8.01–7.95 (m, 2H), 7.12 (d, J = 8.9 Hz, 1H), 4.98 (q, J = 8.5 Hz, 2H), 4.35 (s, 2H), 3.15 (s, 2H), 1.05 (s, 6H); MS (ESI) 447.5 m/z [MH+], $C_{21}H_{21}F_3N_6O_2$ requires 447.4.

2-((4-Amino-3-(6-cyclopropoxynaphthalen-2-yl)-1H-pyrazolo[3,4-d]pyrimidin-1-yl)methyl)-1,1,1,3,3,3-hexafluoropropan-2-ol (37): 2-(6-Cyclopropoxynaphthalen-2-yl)-4,4,5,5-tetramethyl-1,3,2-dioxaborolane (**41**) and 2-((4-amino-3-iodo-1*H*-pyrazolo[3,4-*d*]pyrimidin-1-yl)methyl)-1,1,1,3,3,3-hexafluoropropan-2-ol (**45**) were subjected to the *General Suzuki coupling procedure* in order to afford **37**. ^{1}H NMR (300 MHz, CD$_3$OD) δ 8.32 (s, 1H), 8.11 (s, 1H), 7.97 (d, *J* = 8.5 Hz, 1H), 7.87 (d, *J* = 9.1 Hz, 1H), 7.76 (dd, *J* = 8.5, 1.6 Hz, 1H), 7.59 (d, *J* = 2.0, 1H), 7.23 (dd, *J* = 8.9, 2.2 Hz, 1H), 5.03 (s, 2H), 3.94 (m, 1H), 0.94–0.76 (m, 4H); MS (ESI) 498.2 *m/z* [MH+], C$_{22}$H$_{18}$F$_6$N$_5$O$_2$ requires 498.2.

Physiochemical Procedures

Pharmacokinetic analysis in mice—For mouse oral PK studies, three female BALB/c mice (10 to 12 weeks old) were used in each group (performed under IACUC protocol number 2145-01 (UW, Seattle)). Each group received a test compound at a dose of 10 mg/kg body weight dissolved in 3% ethanol/7% Tween 80/90% normal saline by oral gavage. Blood samples were taken at the designated time points by tail bleeding and centrifuged to obtain plasma. The samples were frozen at −20 °C. The test compounds were extracted from the plasma samples using acetonitrile/0.1% formic acid with an internal standard. A standard mix of all test compounds was prepared for comparison and quantification. The compounds were quantified by LC/MS analysis. PK calculations were performed using Phoenix WinNonlin software (Pharsight).

Pharmacokinetic analysis in rats—Test compound was administered to Sprague-Dawley jugular canulated rats (Charles River) by either oral gavage or IV injection followed by blood sampling from the jugular vein at designated time points (performed under IACUC protocol number 2145-01 (UW, Seattle)). The oral dose was administered to each rat at 20 mg/kg for compound **32** and 5 mg/kg for compound **33** at time = 0 in a 1 mL volume of dosing solution (7% Tween 80, 3% EtOH, 5% DMSO, 0.9% saline.) IV injections were administered at 5 mg/kg from time = 0 to 3 minutes in a 1 mL volume of dosing solution, and blood was sampled at the same time points via the jugular vein. Experiments were performed with groups of 2 rats each for the oral and IV dosing. Plasma was separated and extracted with acetonitrile and quantified by LC/MS analysis. PK calculations were performed using Phoenix WinNonlin software (Pharsight).

Pharmacokinetic analysis in calves—Previously described procedures were used for calf enrollment, housing, management, and for test compound administration (performed under WSU IACUC # ASAF 04477 "Novel Therapeutics for Cryptosporidiosis and other Parasites: Bumped Kinase Inhibitors").[36]

Pharmacokinetic analysis in dogs and monkeys—In each study, groups of three animals received a 1 mg/kg intravenous or oral dose of compound **32**. The dose was administered as a solution in PEG-400 containing 10% DMSO (0.5 ml/kg dose volume); the oral dose solution was placed in a capsule just prior to dosing. Blood samples for plasma concentration analysis were obtained from each animal for 24 hours after dosing. Plasma concentrations of parent drug were determined by LC-MS/MS. All studies involving

vertebrate animals at AbbVie were approved by an animal ethics approval committee (IACUC).

Distribution of compounds between mouse plasma and brain—Mice were injected with **32** or **33** (5 mg/kg IP) and sacrificed at the indicated times for collection of plasma and brain (performed under IACUC protocol number 2145-01 (UW, Seattle)). Compound was dissolved in 0.4 mL of dosing solution (7% Tween 80, 3% ethanol, 5% DMSO, 0.9% saline) for IP injections. The brains were weighed and immediately frozen, then later homogenized in acetonitrile. Prior to animal studies, recovery of test compound was carried out by adding a known amount to a mouse brain in the test extraction solvent and performing the homogenization. Compound recovery was determined by liquid chromatography/tandem mass spectrometry analysis relative to a standard compound amount. Blood was taken from the same mice in heparinized capillary tubes for determination of compound concentration in plasma. The concentration of compound in the brain was obtained by dividing the moles of compound in the brain by the brain volume (obtained from the brain weight assuming 1 g is 1 mL) and correcting for the brain vasculature volume of 3% by weight.

Supplementary Material

Refer to Web version on PubMed Central for supplementary material.

Acknowledgments

ABBREVIATIONS USED

AUC	area under plasma concentration time curve
ATP	adenosine triphosphate
Boc	*tert*-butyloxycarbonyl
CDPK1	calcium-dependent protein kinase 1
CL	clearance
Cmax	maximum plasma concentration

CNS	central nervous system
DIAD	diisopropyl azodicarboxylate
DMF	dimethylformamide
dppf	1,1′-bis(diphenylphosphino)ferrocene
EC$_{50}$	half maximal effective concentration
GI$_{50}$	half maximal growth inhibition
hERG	human Ether-à-go-go-Related Gene
IC$_{50}$	half maximal inhibitory concentration
IV	intravenous
K$_{m}$	Michaelis constant
PO	*per os*
tmax	time at which maximum concentration is reached
TBDMS	*tert*-butyldimethylsilyl
***Tg*CDPK1**	*Toxoplasma gondii* CDPK1

References

1. Tenter AM, Heckeroth AR, Weiss LM. Toxoplasma gondii: from animals to humans. Int J Parasitol. 2000; 30:1217–1258. [PubMed: 11113252]

2. Pappas G, Roussos N, Falagas ME. Toxoplasmosis snapshots: global status of Toxoplasma gondii seroprevalence and implications for pregnancy and congenital toxoplasmosis. Int J Parasitol. 2009; 39:1385–1394. [PubMed: 19433092]

3. Schwartzman, JD.; Maguire, JH. In Tropical Infectious Diseases: Principles, Pathogens and Practice. 3rd. W. B. Saunders; Edinburgh, U.K.: 2011. Toxoplasmosis; p. 722-728.Chapter 103

4. Dupont CD, Christian DA, Hunter CA. Immune response and immunopathology during toxoplasmosis. Semin Immunopathol. 2012; 34:793–813. [PubMed: 22955326]

5. Blanchard N, Dunay IR, Schluter D. Persistence of *Toxoplasma gondii* in the central nervous system: a fine-tuned balance between the parasite, the brain and the immune system. Parasite Immunol. 2015; 37:150–158. [PubMed: 25573476]

6. Flegr J, Prandota J, Sovickova M, Israili ZH. Toxoplasmosis-a global threat. Correlation of latent toxoplasmosis with specific disease burden in a set of 88 countries. PLoS One. 2014; 9:e90203. [PubMed: 24662942]

7. Jones JL, Muccioli C, Belfort R Jr, Holland GN, Roberts JM, Silveira C. Recently acquired *Toxoplasma gondii* infection, Brazil. Emerging Infect Dis. 2006; 12:582–587. [PubMed: 16704805]

8. Carlier Y, Truyens C, Deloron P, Peyron F. Congenital parasitic infections: a review. Acta Trop. 2012; 121:55–70. [PubMed: 22085916]

9. Dubey JP, Jones JL. *Toxoplasma gondii* infection in humans and animals in the United States. Int J Parasitol. 2008; 38:1257–1278. [PubMed: 18508057]

10. Wei HX, Wei SS, Lindsay DS, Peng HJ. A Systematic Review and Meta-Analysis of the Efficacy of Anti-*Toxoplasma gondii* Medicines in Humans. PLoS One. 2015; 10:e0138204. [PubMed: 26394212]

11. Kaplan JE, Benson C, Holmes KK, Brooks JT, Pau A, Masur H, Centers for Disease Control and Prevention (CDC); NIH Publ. HIV Medicine Asso. of the Infect. Dis. Soc. of America Guidelines for prevention and treatment of opportunistic infections in HIV-infected adults and adolescents: recommendations from CDC, the National Institutes of Health, and the HIV Medicine Association of the Infectious Diseases Society of America. MMWR. 2009; 58:1–207.

12. Kieschnick H, Wakefield T, Narducci CA, Beckers C. *Toxoplasma gondii* attachment to host cells is regulated by a calmodulin-like domain protein kinase. J Biol Chem. 2001; 276:12369–12377. [PubMed: 11154702]

13. Lourido S, Shuman J, Zhang C, Shokat KM, Hui R, Sibley LD. Calcium-dependent protein kinase 1 is an essential regulator of exocytosis in Toxoplasma. Nature. 2010; 465:359–362. [PubMed: 20485436]

14. Lourido S, Zhang C, Lopez MS, Tang K, Barks J, Wang Q, Wildman SA, Shokat KM, Sibley LD. Optimizing small molecule inhibitors of calcium-dependent protein kinase 1 to prevent infection by *Toxoplasma gondii*. J Med Chem. 2013; 56:3068–3077. [PubMed: 23470217]

15. Doggett JS, Ojo KK, Fan E, Maly DJ, Van Voorhis WC. Bumped kinase inhibitor 1294 treats established *Toxoplasma gondii* infection. Antimicrob Agents Chemother. 2014; 58:3547–3549. [PubMed: 24687502]

16. Zhang Z, Ojo KK, Johnson SM, Larson ET, He P, Geiger JA, Castellanos-Gonzalez A, White AC Jr, Parsons M, Merritt EA, Maly DJ, Verlinde CL, Van Voorhis WC, Fan E. Benzoylbenzimidazole-based selective inhibitors targeting *Cryptosporidium parvum* and *Toxoplasma gondii* calcium-dependent protein kinase-1. Bioorg Med Chem Lett. 2012; 22:5264–5267. [PubMed: 22795629]

17. Zhang Z, Ojo KK, Vidadala R, Huang W, Geiger JA, Scheele S, Choi R, Reid MC, Keyloun KR, Rivas K, Siddaramaiah LK, Comess KM, Robinson KP, Merta PJ, Kifle L, Hol WG, Parsons M, Merritt EA, Maly DJ, Verlinde CL, Van Voorhis WC, Fan E. Potent and selective inhibitors of CDPK1 from *T. gondii* and *C. parvum* Based on a 5-aminopyrazole-4-carboxamide scaffold. ACS Med Chem Lett. 2014; 5:40–44. [PubMed: 24494061]

18. Murphy RC, Ojo KK, Larson ET, Castellanos-Gonzalez A, Perera BG, Keyloun KR, Kim JE, Bhandari JG, Muller NR, Verlinde CL, White AC Jr, Merritt EA, Van Voorhis WC, Maly DJ. Discovery of Potent and Selective Inhibitors of Calcium-Dependent Protein Kinase 1 (CDPK1) from *C. parvum* and *T. gondii*. ACS Med Chem Lett. 2010; 1:331–335. [PubMed: 21116453]

19. Johnson SM, Murphy RC, Geiger JA, DeRocher AE, Zhang Z, Ojo KK, Larson ET, Perera BG, Dale EJ, He P, Reid MC, Fox AM, Mueller NR, Merritt EA, Fan E, Parsons M, Van Voorhis WC, Maly DJ. Development of *Toxoplasma gondii* calcium-dependent protein kinase 1 (*Tg*CDPK1) inhibitors with potent anti-toxoplasma activity. J Med Chem. 2012; 55:2416–2426. [PubMed: 22320388]

20. Ojo KK, Larson ET, Keyloun KR, Castaneda LJ, Derocher AE, Inampudi KK, Kim JE, Arakaki TL, Murphy RC, Zhang L, Napuli AJ, Maly DJ, Verlinde CL, Buckner FS, Parsons M, Hol WG, Merritt EA, Van Voorhis WC. *Toxoplasma gondii* calcium-dependent protein kinase 1 is a target for selective kinase inhibitors. Nat Struct Mol Biol. 2010; 17:602–607. [PubMed: 20436472]

21. Ojo KK, Reid MC, Kallur Siddaramaiah L, Muller J, Winzer P, Zhang Z, Keyloun KR, Vidadala RS, Merritt EA, Hol WG, Maly DJ, Fan E, Van Voorhis WC, Hemphill A. *Neospora caninum* calcium-dependent protein kinase 1 is an effective drug target for neosporosis therapy. PLoS One. 2014; 9:e92929. [PubMed: 24681759]

22. Winzer P, Muller J, Aguado-Martinez A, Rahman M, Balmer V, Manser V, Ortega-Mora LM, Ojo KK, Fan E, Maly DJ, Van Voorhis WC, Hemphill A. *In Vitro* and *In Vivo* Effects of the Bumped Kinase Inhibitor 1294 in the Related Cyst-Forming Apicomplexans *Toxoplasma gondii* and *Neospora caninum*. Antimicrob Agents Chemother. 2015; 59:6361–6374. [PubMed: 26248379]

23. Ojo KK, Eastman RT, Vidadala R, Zhang Z, Rivas KL, Choi R, Lutz JD, Reid MC, Fox AM, Hulverson MA, Kennedy M, Isoherranen N, Kim LM, Comess KM, Kempf DJ, Verlinde CL, Su XZ, Kappe SH, Maly DJ, Fan E, Van Voorhis WC. A specific inhibitor of *Pf*CDPK4 blocks malaria transmission: chemical-genetic validation. J Infect Dis. 2014; 209:275–284. [PubMed: 24123773]

24. van Noord C, Eijgelsheim M, Stricker BH. Drug- and non-drug-associated QT interval prolongation. Br J Clin Pharmacol. 2010; 70:16–23. [PubMed: 20642543]

25. Larson ET, Ojo KK, Murphy RC, Johnson SM, Zhang Z, Kim JE, Leibly DJ, Fox AM, Reid MC, Dale EJ, Perera BG, Kim J, Hewitt SN, Hol WG, Verlinde CL, Fan E, Van Voorhis WC, Maly DJ, Merritt EA. Multiple determinants for selective inhibition of apicomplexan calcium-dependent protein kinase CDPK1. J Med Chem. 2012; 55:2803–2810. [PubMed: 22369268]

26. Vidadala RS, Ojo KK, Johnson SM, Zhang Z, Leonard SE, Mitra A, Choi R, Reid MC, Keyloun KR, Fox AM, Kennedy M, Silver-Brace T, Hume JC, Kappe S, Verlinde CL, Fan E, Merritt EA, Van Voorhis WC, Maly DJ. Development of potent and selective *Plasmodium falciparum* calcium-dependent protein kinase 4 (*Pf*CDPK4) inhibitors that block the transmission of malaria to mosquitoes. Eur J Med Chem. 2014; 74:562–573. [PubMed: 24531197]

27. Hanke JH, Gardner JP, Dow RL, Changelian PS, Brissette WH, Weringer EJ, Pollok BA, Connelly PA. Discovery of a novel, potent, and Src family-selective tyrosine kinase inhibitor. Study of Lck- and FynT-dependent T cell activation. J biol chem. 1996; 271:695–701. [PubMed: 8557675]

28. Bridal TR, Margulis M, Wang X, Donio M, Sorota S. Comparison of human Ether-a-go-go related gene screening assays based on IonWorks Quattro and thallium flux. Assay Drug Dev Technol. 2010; 8:755–765. [PubMed: 20658944]

29. Bowes J, Brown AJ, Hamon J, Jarolimek W, Sridhar A, Waldron G, Whitebread S. Reducing safety-related drug attrition: the use of *in vitro* pharmacological profiling. Nat Rev Drug Discov. 2012; 11:909–22. [PubMed: 23197038]

30. Hitchcock SA, Pennington LD. Structure-brain exposure relationships. J Med Chem. 2006; 49:7559–7583. [PubMed: 17181137]

31. Cheng Y, Brown J, Judd TC, Lopez P, Qian W, Powers TS, Chen JJ, Bartberger MD, Chen K, Dunn RT, Epstein O, Fremeau RT Jr, Harried S, Hickman D, Hitchcock SA, Luo Y, Minatti AE, Patel VF, Vargas HM, Wahl RC, Weiss MM, Wen PH, White RD, Whittington DA, Zheng XM, Wood S. An Orally Available BACE1 Inhibitor That Affords Robust CNS Aβ Reduction without Cardiovascular Liabilities. ACS Med Chem Lett. 2015; 6:210–215. [PubMed: 25699151]

32. Epstein O, Bryan MC, Cheng AC, Derakhchan K, Dineen TA, Hickman D, Hua Z, Human JB, Kreiman C, Marx IE, Weiss MM, Wahl RC, Wen PH, Whittington DA, Wood S, Zheng XM, Fremeau RT Jr, White RD, Patel VF. Lead optimization and modulation of hERG activity in a series of aminooxazoline xanthene β-site amyloid precursor protein cleaving enzyme (BACE1) inhibitors. J Med Chem. 2014; 57:9796–9810. [PubMed: 25389560]

33. Keyloun KR, Reid MC, Choi R, Song Y, Fox AM, Hillesland HK, Zhang Z, Vidadala R, Merritt EA, Lau AO, Maly DJ, Fan E, Barrett LK, WC VANV, Ojo KK. The gatekeeper residue and beyond: homologous calcium-dependent protein kinases as drug development targets for veterinarian Apicomplexa parasites. Parasitology. 2014; 141:1499–1509. [PubMed: 24927073]

34. Doggett JS, Nilsen A, Forquer I, Wegmann KW, Jones-Brando L, Yolken RH, Bordón C, Charman SA, Katneni K, Schultz T, Burrows JN, Hinrichs DJ, Meunier B, Carruthers VB, Riscoe MK. Endochin-like quinolones are highly efficacious against acute and latent experimental toxoplasmosis. Proc Natl Acad Sci USA. 2012; 109:15936–15941. [PubMed: 23019377]

35. Edvinsson B, Lappalainen M, Evengård B, ESCMID Study Group for Toxoplasmosis. Real-time PCR targeting a 529-bp repeat element for diagnosis of toxoplasmosis. Clin Microbiol Infect. 2006; 12:131–136. [PubMed: 16441450]

36. Ollivett TL, Nydam DV, Bowman DD, Zambriski JA, Bellosa ML, Linden TC, Divers TJ. Effect of nitazoxanide on cryptosporidiosis in experimentally infected neonatal dairy calves. J Dairy Sci. 2009; 92:1643–1648. [PubMed: 19307646]
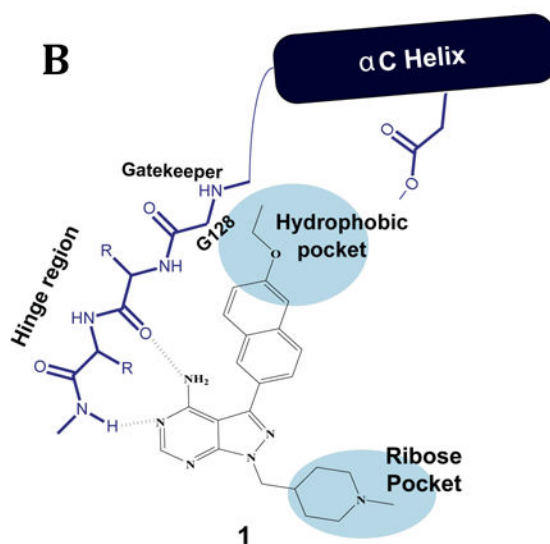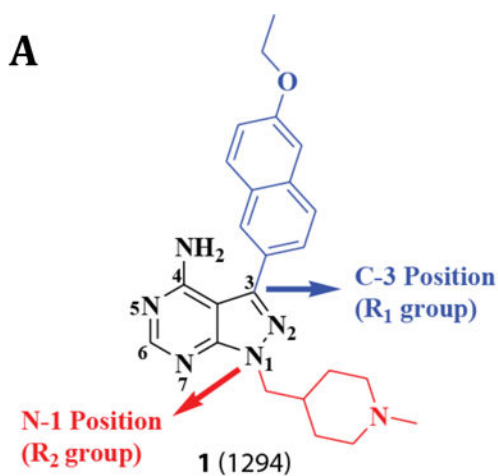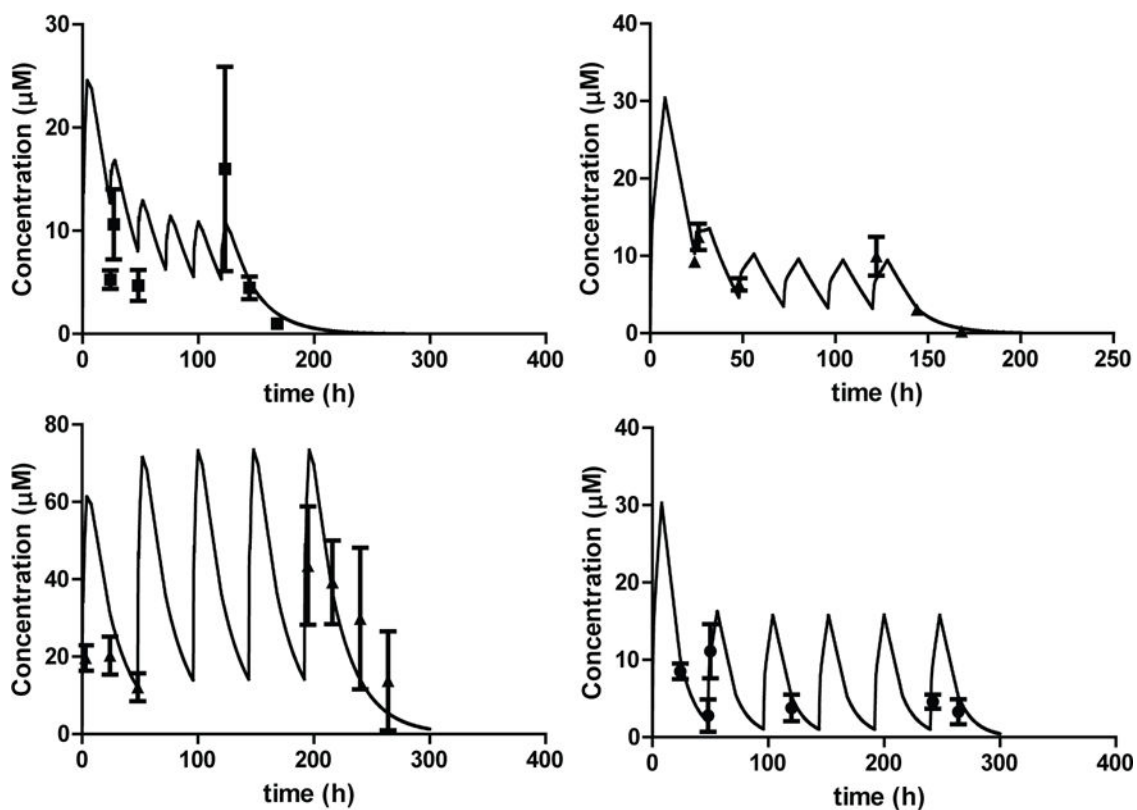
Figure 1.
Inhibitor **1**. (A) The chemical structure of compound **1**. Pyrazolopyrimidine scaffold numbering and sites of inhibitor derivatization (R_1 and R_2) are shown. (B) Schematic of how 1 interacts with the ATP-binding site of *Tg*CDPK1.
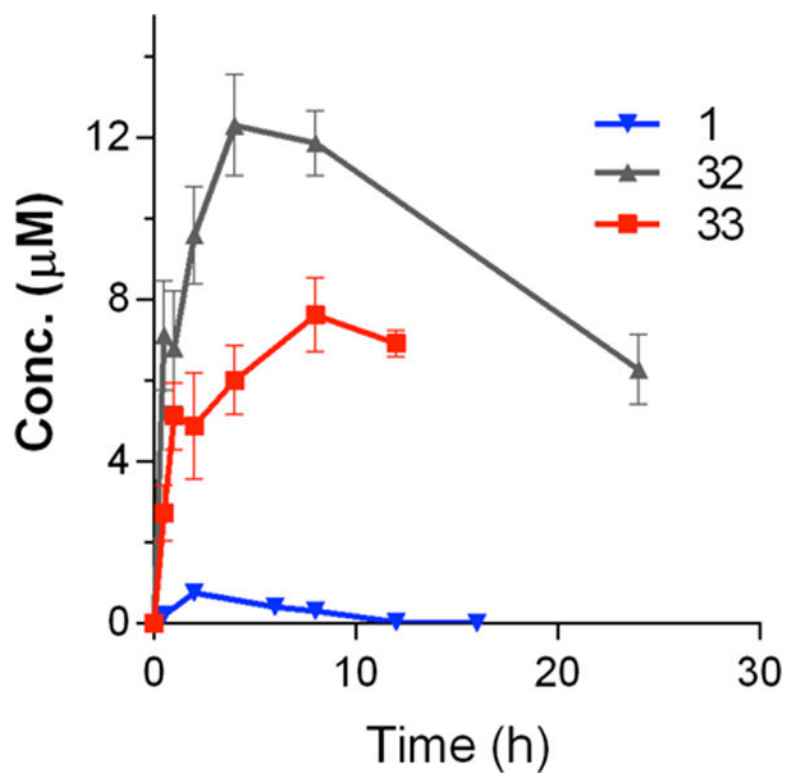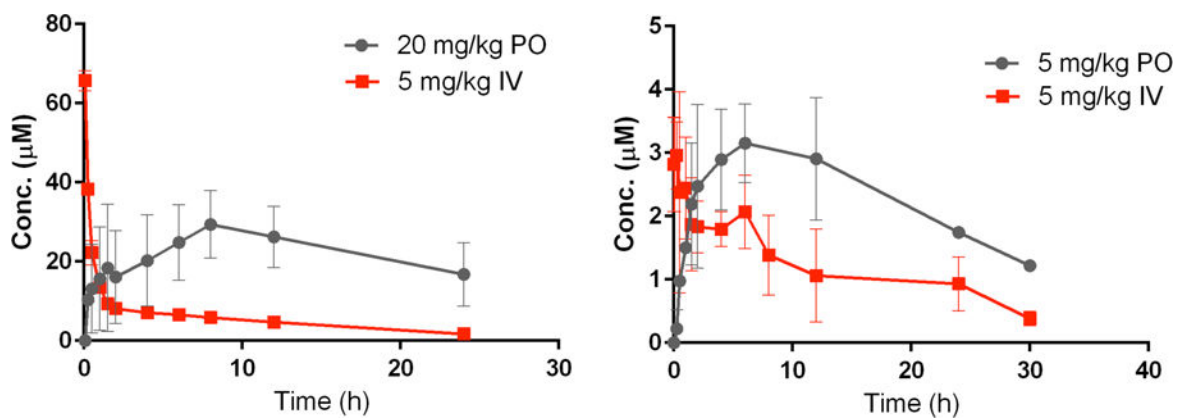
Figure 2.
Comparison of oral PK for compounds **32** and **33** in mice. Both compounds were dosed at 10 mg/kg, PO.
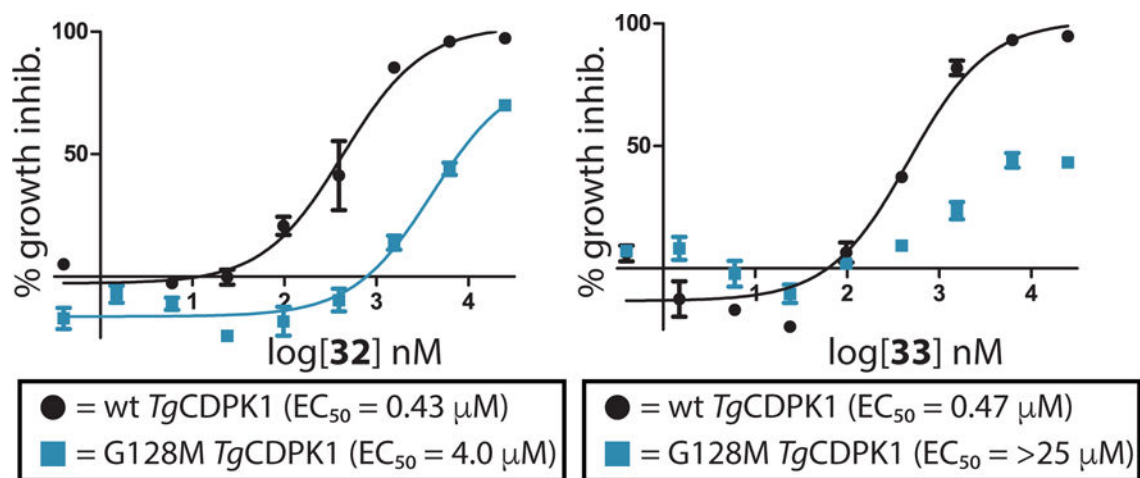
Figure 3.
Multiple dose PK studies with compound **32** and **33**. The dosing regimens were simulated based on the disposition data following single oral doses to mice (lines) and the observed plasma concentrations (dots) compared to the simulation. (*top left panel*) **32** was dosed at 20 mg/kg on day 1 and then 5 mg/kg every 24 hours for 5 doses. (*bottom left panel*) **32** was dosed at 50 mg/kg every 48 hours for 5 doses. (*top right panel*) **33** was dosed at 20 mg/kg on day 1 and then 5 mg/kg every 24 hours for 5 doses. (*bottom right panel*) **33** was dosed at 20 mg/kg on day 1 and then 10 mg/kg every 48 hours for 5 doses. Each dot is a mean of 3 mice with standard deviation.

Figure 4.
Plasma concentration time curves for compound **32** (left) and **33** (right) following IV and PO dosing to rats.

Figure 5.
EC$_{50}$ curves of inhibitors **32** (left) and **33** (right) for *T. gondii* over-expressing either wild type (wt) *Tg*CDPK1 (black circles) or a drug resistant G128M *Tg*CDPK1 mutant (blue squares). All experiments were performed in triplicate.
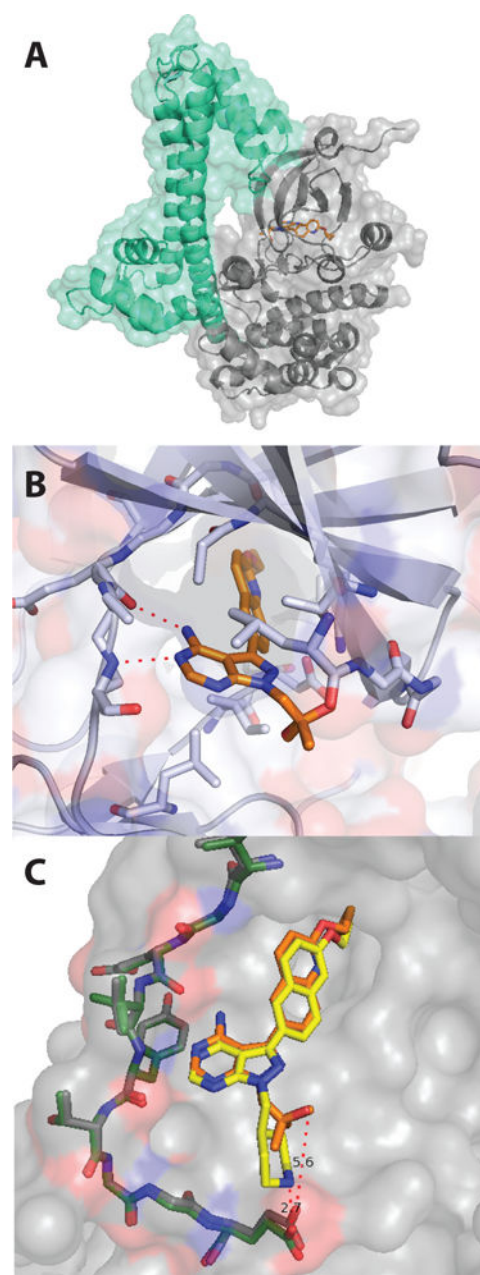
Figure 6.
Structure of the *Tg*CDPK1·**33** complex (PDB accession code: 4TZR). (A) Entire view of the **33·***Tg*CDPK1 co-crystal structure. Inhibitor **33** is shown as orange sticks. The CDPK activation domain (CAD) of *Tg*CDPK1 is in mint and the kinase domain is shown in grey. (B) Expanded view of the ATP-binding site from the *Tg*CDPK1·**33** complex. The backbone amides of residues Glu129 and Tyr131 in the hinge region (shown as sticks) form two hydrogen bonds (dashed red lines) with the pyrazolopyrimidine scaffold of **33**. The 2-cyclopropyloxyquinolin-6-yl R_2 group of **33** is directed towards the Gly128 gatekeeper residue. (C) An overlay of an analog of **1** (yellow) bound to *Tg*CDPK1 (PDB accession code: 3SX9) and the *Tg*CDPK1·**33** (orange) complex (PDB accession code: 3SX9)
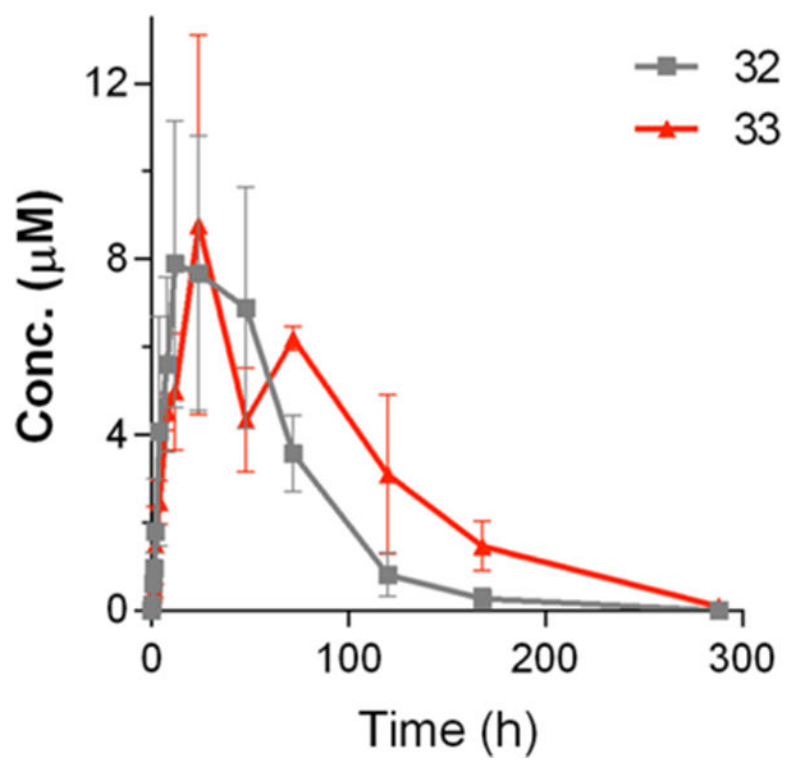
Figure 7.
Calf plasma levels. Comparison of oral PK for compounds **32** and **33**. Each compound was tested in two calves. Compounds **32** was dosed at 9.3 mg/kg and compound **33** was dosed at 10 mg/kg, PO. Each point shows the mean and range of measurements in two calves.
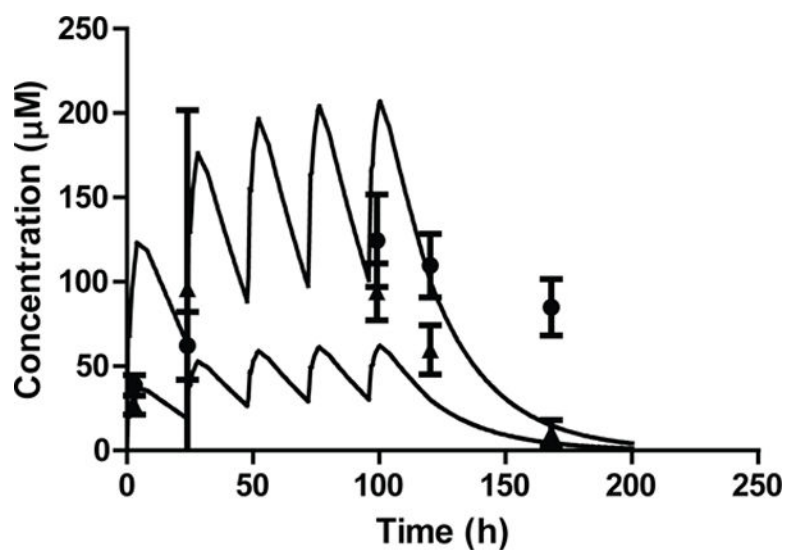
Figure 8.
Exposure to compound **32** in multiple dose toxicity studies. The concentration profiles of **32** following 30 mg/kg and 100 mg/kg daily doses were simulated based on the single dose 10 mg/kg data. The mean observed concentrations (n=3) with standard deviation are plotted as triangles for 30 mg/kg dosing and circles for the 100 mg/kg dosing) with the simulation.
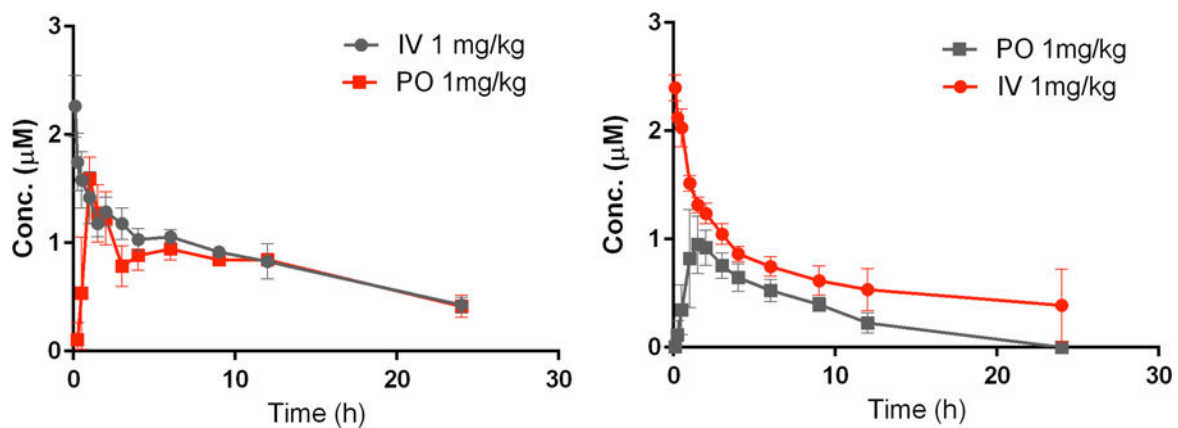
Figure 9.
Plasma concentration time curves for compound **32** following IV and PO dosing to dogs (left) and monkeys (right).
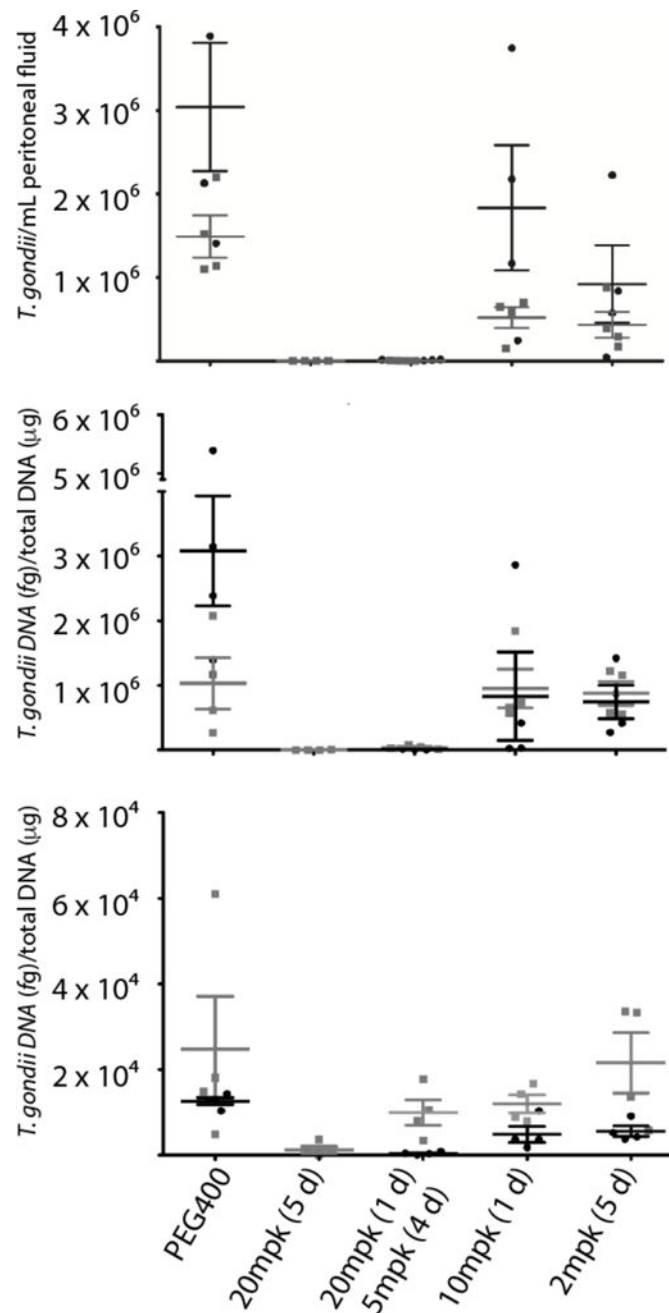
Figure 10.
Inhibitor **32** is efficacious against acute toxoplasmosis. Efficacy was evaluated by measurement of *T. gondii* in peritoneal fluid (top), spleen (middle), and brain (bottom) in two experiments. Mice were treated daily for 5 days, beginning 2 days after IP infection with *T. gondii.* Mice were analyzed one day after the last dose. Peritoneal fluid was analyzed by fluorescent microscopy and spleen and brain tissue were analyzed by quantitative real-time PCR. Groups consisted of 4 mice. Bars represent the mean and the standard error of the mean. PEG = polyethylene glycol; mpk = mg/kg.
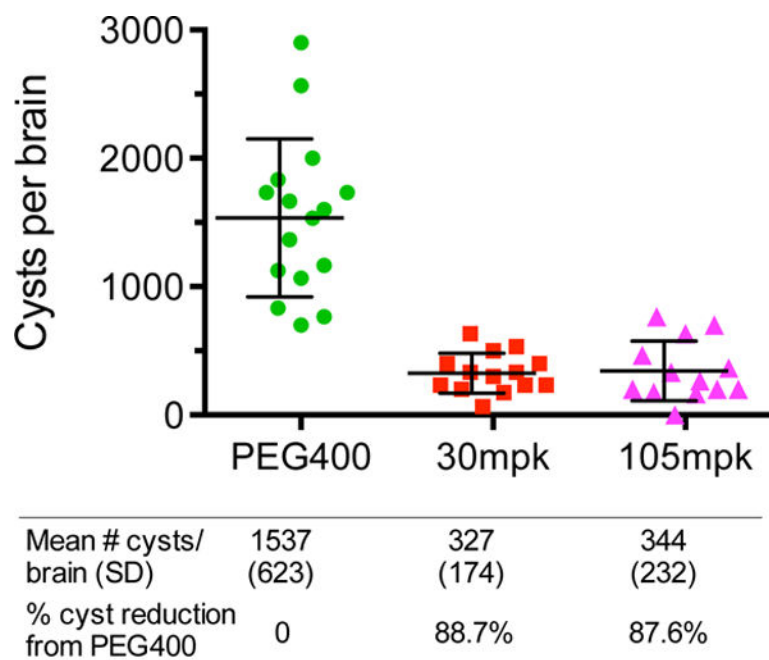
Fig. 11.
Inhibitor **32** is efficacious against latent *T. gondii* infection. **32** reduced the number of *T. gondii* cysts per brain compared to a vehicle control. Five weeks after being inoculated by the ME49 *T. gondii* strain, mice were treated once daily for 14 days *via* oral gavage with 30 mg/kg of **32** or PEG400 vehicle control. A group of mice was also treated twice–days 1 and 7–via oral gavage with 105 mg/kg of **32**. Two weeks after the final drug treatment, mice were sacrificed and the number of brain cysts was determined. The number of cysts per brain was >85% lower for both dosing regimens of **32** relative to a vehicle control. Bars represent the mean and the standard error of the mean. PEG = polyethylene glycol; mpk = mg/kg.
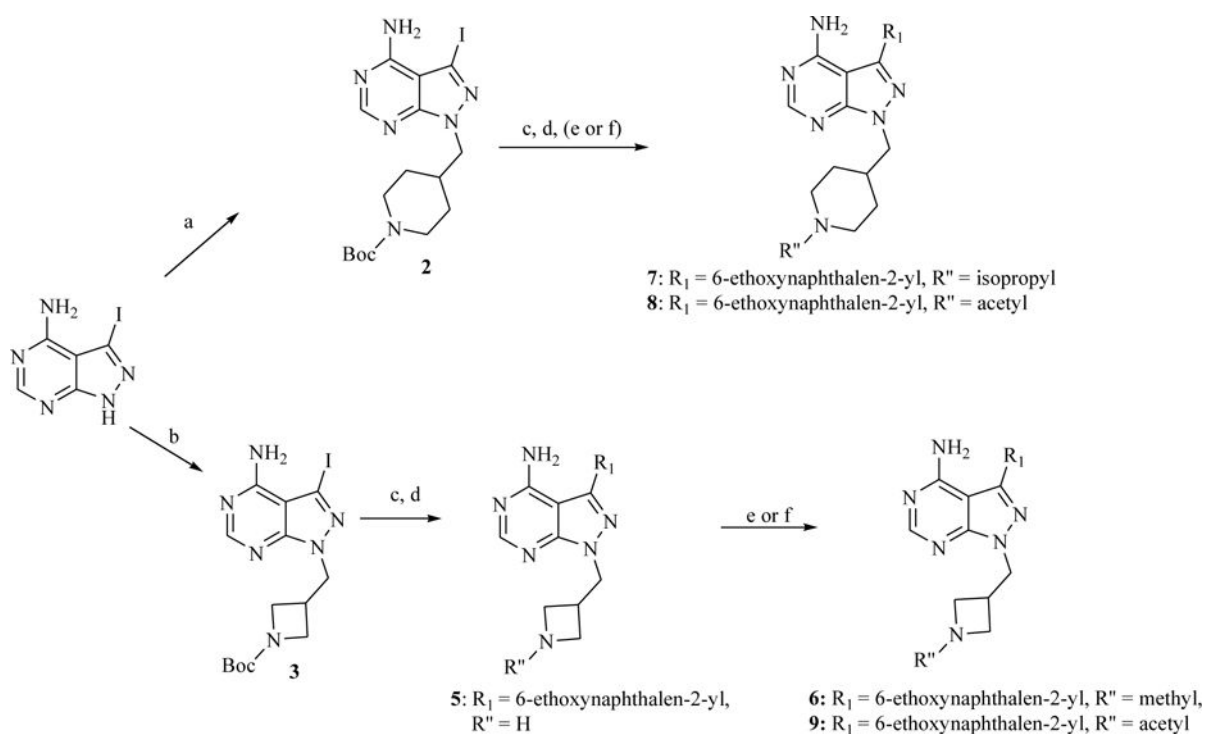
Scheme 1.

a) *N*-Boc-4-piperidinemethanol mesylate, Cs_2CO_3, DMF, 80 °C; b) *N*-Boc-3-azetidinemethanol mesylate, Cs_2CO_3, DMF, 80 °C; c) Na_2CO_3, Pd(PPh$_3$)$_4$, 6-ethoxy-2-naphthaleneboronic acid, H_2O/DME, 80 °C (microwave); d) TFA/CH_2Cl_2 (1:1); e) sodium methoxide in MeOH, then 2% AcOH, formaldehyde or acetone, $NaBH_3CN$; f) Ac_2O, TEA, DMF.
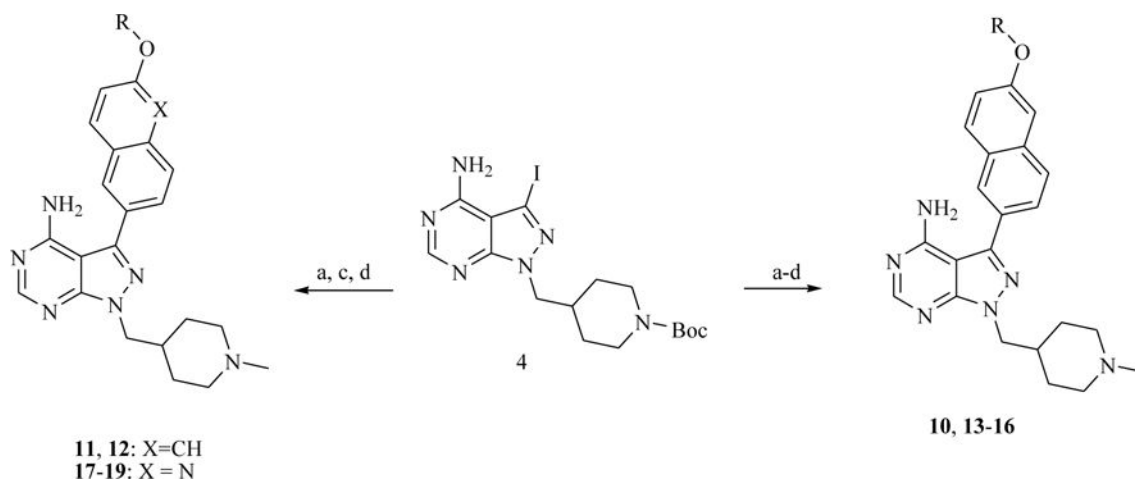
Scheme 2.
a) aryl boronate ester, K_3PO_4/Na_2CO_3, $PdCl_2$(dppf), 1,4-Dioxane:H_2O or DME:H_2O, 80 °C (microwave); b) alkyl halide or epoxide, NaH_2PO_4:K_2CO_3 (1:1), DMF, 60 °C; c) TFA/ CH_2Cl_2 (1:1); d) sodium methoxide in MeOH, then 2% AcOH, formaldehyde, $NaBH_3CN$. Compound **4** was synthesized according to a previously reported procedure.[19]
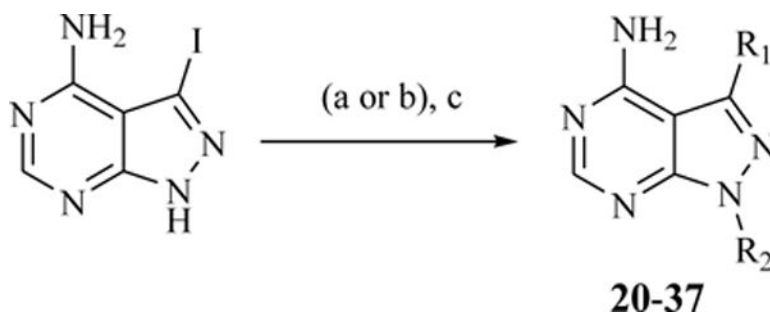
Scheme 3.

a) alkyl halide or alkyl mesylate, Cs_2CO_3, DMF, 80 °C; b) epoxide, NaH_2PO_4:K_2CO_3 (1:1), DMF, 80 °C; c) aryl boronate ester, K_3PO_4 or Na_2CO_3, $PdCl_2$(dppf) or $Pd(PPh_3)_4$, 1,4-Dioxane:H_2O or DME:H_2O, 80 °C (microwave).
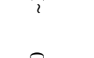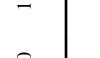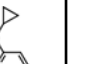
Table 1

Enzymatic *Tg*CDPK1 and Src inhibition (IC$_{50}$), hERG inhibition (IC$_{50}$), HepG2 and CRL-8155 growth inhibition (GI$_{50}$) and *T. gondii* cellular assay (EC$_{50}$) results for compounds with variable R$_2$ substructures (**1**–**9**). IC$_{50}$ and GI$_{50}$ values are the averages of at least three assays. *T. gondii* cellular assay EC$_{50}$ values are the average of at least two runs that were performed in triplicate.

R$_2$	IC$_{50}$ (µM)			human cells, GI$_{50}$ (µM)		EC$_{50}$ (µM)
	*Tg*CDPK1	Src	hERG	HepG2	CRL-8155	*T. gondii*
1	0.0029	>10	0.40	>10	>10	0.14
5	0.0032	>10	1.7	>10	>10	0.283
6	0.0060	>10	1.4	>10	>10	0.41
7	0.010	>10	0.30	>10	>10	0.51
8	0.011	>10	>10	>10	>10	0.22
9	0.004	1.1	>10	>10	>10	0.48

Table 2

Enzymatic *TgCDPK1* and Src inhibition (IC$_{50}$), hERG inhibition (IC$_{50}$), HepG2 and CRL-8155 growth inhibition (GI$_{50}$) and *T. gondii* cellular assay (EC$_{50}$) results for compounds with variable R$_1$ substructures (**10–19**). IC$_{50}$ and GI$_{50}$ values are the averages of at least three assays. *T. gondii* cellular assay EC$_{50}$ values are the average of at least two runs that were performed in triplicate. Compounds that did not show an IC$_{50}$ < 0.010 μM for *TgCDPK1* or an IC$_{50}$ > 5 μM for hERG were de-prioritized for further testing.

R$_1$	IC$_{50}$ (μM)			human cells, GI$_{50}$ (μM)		EC$_{50}$ (μM)
	TgCDPK1	Src	*hERG*	HepG2	CRL-8155	*T. gondii*
1	0.0029	>10	0.40	>10	>10	0.14
10	0.0040	>10	0.90	>10	>10	0.61
11	0.0025	>10	0.20	>10	>10	0.32
12	0.0015	>10	0.37	–	>10	0.12
13	0.015	>10	–	>10	>10	0.71
14	0.010	>10	–	>10	>10	–
15	0.046	–	–	–	–	–
16	0.024	>10	–	>10	>10	–

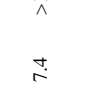| R₁	IC₅₀ (µM)			human cells, GI₅₀ (µM)		EC₅₀ (µM)
	TgCDPK1	Src	hERG	HepG2	CRL-8155	T. gondii
17	0.0061	>10	~10	>10	>10	0.27
18	0.0022	–	0.50	–	–	0.33
19	0.0016	>10	1.7	>10	–	0.098
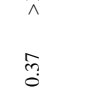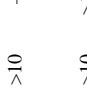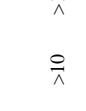
–Not tested

Table 3

Enzymatic $TgCDPK1$ and Src inhibition (IC_{50}), hERG inhibition (IC_{50}), HepG2 and CRL-8155 growth inhibition (GI_{50}) and *T. gondii* cellular assay (EC_{50}) results for compounds with variable R_1 and R_2 substructures (**20–37**). IC_{50} and GI_{50} values are the averages of at least three assays. *T. gondii* cellular assay EC_{50} values are the average of at least two runs that were performed in triplicate.

R_2	R_1		IC$_{50}$ (µM)			human cells, GI$_{50}$ (µM)		EC$_{50}$ (µM)
			TgCDPK1	Src	hERG	HepG2	CRL-8155	*T. gondii*
	1		0.0029	>10	0.40	>10	>10	0.14
	20		0.0045	>10	0.082	>10	>10	0.26
	21		0.00080	>10	>10	>10	>10	0.12
	22		0.0011	3.7	>10	–	>10	0.071
	23		0.0012	>10	>10	>10	>10	0.090
	24		0.0021	>10	1.9	>10	>10	0.045
	25		0.0018	>10	>10	>10	>10	0.21
	26		0.0020	>10	>10	>10	>10	0.076
	27		0.0020	>10	>10	>10	>10	0.078

R₂	R₁	IC$_{50}$ (µM)			human cells, GI$_{50}$ (µM)		EC$_{50}$ (µM)
		TgCDPK1	*Src*	*hERG*	HepG2	CRL-8155	*T. gondii*
28		0.0024	0.37	>10	>10	>10	0.077
29		0.0018	>10	>10	>10	>10	0.081
30		0.0056	>10	–	>10	>10	0.75
31		0.0033	>10	>10	>10	>10	0.17
32		0.001	>10	>10	>10	>10	0.060
33		0.002	>10	>10	>10	>10	0.16
34		0.00090	3.1	>10	>10	>10	0.056
35		0.0013	7.4	>10	>10	>10	0.018
36		0.017	>10	–	>10	>10	0.70
37		0.094	>10	–	>10	>10	–

–Not tested

Table 4

Solubility (in phosphase-buffered saline, pH= 6.5) and PK properties of the most potent and selective *Tg*CDPK1 inhibitors dosed at 10 mg/kg PO to mice.

	Solubility (μM)	T_{max} (min)	C_{max} (μM)	$AUC_{o->inf}$ (μM.min)	Half life (min)	clearance (mL/min)
1	82	120	0.75 ±0.15	430 ±58	233 ±26	0.7
8	48	50	0.89 ±0.17	94 ±51	68 ±64	2.5
17	54	200	0.26 ±0.04	128 ± 53	223 ±182	1.8
29	17	30	0.88 ±0.23	67 ±60	50 ±73	110
31	>100	50	5.2 ±1.0	850 ± 411	114 ±115	0.2
32	>100	320	13 ±1	13700 ±1500	1190 ±510	0.2
33	>100	560	7.8 ±1.4	16600 ±4300	1110 ±400	0.3
34	6.2	40	0.39 ±0.16	31 ±8	40 ±5	6.7
35	8.0	30	3.9 ±1.1	3.9 ±1.1	41 ±21	21

Table 5

In vivo pharmacokinetic parameters of **32** and **33** in rats following IV administration of 5 mg/kg. Data is shown as mean and range between animals.

	AUC (h*µ mol/L)	*CL (mL/hr/kg)*	*V_{ss} (L/kg)*	*$T_{1/2}$ (hr)*
32	167 (160–175)	77 (73–80)	0.91(0.89–0.93)	9.6 (9.5–9.7)
33	45 (31–59)	310 (216–412)	5.8 (4.1–7.5)	13 (12.6–13.4)

Table 6

In vivo pharmacokinetic parameters of **32** and **33** in calves following PO administration of 10 mg/kg of **32** and 9.3 mg/kg of **33**. Data are shown as the mean and range between animals.

	AUC (h*μ mol/L)	*CL/F (mL/hr/kg)*	*V/F (L/kg)*	*t1/2 (hr)*
32	588 (353–825)	52 (31–72)	1.5 (1.3–1.8)	23 (17–28)
33	849 (607–1091)	30 (22–39)	2.3 (1.4–3.2)	51 (46–56)

Table 7

In vivo pharmacokinetic parameters of **32** following IV and PO administration of 1 mg/kg to dogs and monkeys (n=3 for each). Data is show as mean and standard deviation.

	AUC (h*μ mol/L)	*CL (mL/hr/kg)*	*Vss (L/kg)*	*t1/2 (hr)*
	Dogs			
IV	11200 ±1100	90 ±10	1.7 ±0.1	13.2
PO	9620 ±1350			
	Monkeys			
IV	8720 ±3400	130 ±50	1.8 ±0.3	9.6
PO	5730 ±1500			